

Privacy-protected P2P electricity and carbon emission trading markets based on distributionally robust proximal atomic coordination algorithm

Chengwei Lou ^a, Zekai Jin ^a, Yue Zhou ^b, Wei Tang ^a, Lu Zhang ^{a,*}, Jin Yang ^{c,*}

^a College of Information and Electrical Engineering, China Agricultural University, Beijing, 100083, China

^b School of Engineering, Cardiff University, Cardiff, CF24 3AA, United Kingdom

^c James Watt School of Engineering, University of Glasgow, Glasgow, G12 8QQ, United Kingdom

ARTICLE INFO

Keywords:

P2P energy trading
Distributed optimization
Distributionally robust chance-constrained
Asymmetric nash bargaining
KL divergence
Privacy protection
Carbon emission trading

ABSTRACT

As global power systems modernize towards intelligent infrastructures, peer-to-peer (P2P) energy trading is increasingly adopted worldwide as an innovative electricity market mechanism. This paper explores the decision-making behaviors of diverse agents, market mechanisms, and privacy protections in fully decentralized P2P electricity and carbon emission trading (CET), accounting for uncertainties from renewable energy sources. A novel P2P energy trading mechanism is proposed based on asymmetric Nash bargaining theory. The P2P electricity and carbon market models are decomposed into a cooperative alliance operation problem and an asymmetric cost distribution problem. Additionally, a contribution factor calculation method is introduced, considering both P2P electricity trading and CET marginal effect contribution. To manage renewable energy output uncertainties, a distributionally robust model using Kullback–Leibler (KL) divergence is reformulated as a chance-constrained problem. A proximal atomic coordination (PAC) algorithm is implemented to enhance privacy protection within a fully decentralized framework. Case studies demonstrate that P2P energy trading can reduce total costs by 10.29% and carbon quotas by 11.86% for cooperative alliances. Furthermore, the PAC algorithm decreases total computational time by 12.65% compared to the ADMM algorithm, highlighting its effectiveness in improving computational efficiency and safeguarding user privacy.

1. Introduction

1.1. Background and motivation

As global efforts to modernize and smartify power grids intensify, many countries are adopting peer-to-peer (P2P) energy trading as a key innovation in electricity markets [1]. Traditionally, electricity has been considered a homogeneous commodity, with consumers paying a standardized price regardless of its source. However, P2P trading empowers consumers with greater autonomy and flexibility, promoting local energy production and trading while reducing reliance on centralized grids [2]. It also enhances price transparency and fairness [3]. Moreover, P2P energy trading, which involves high-frequency information exchanges among a diverse set of decentralized agents, increases user participation and decision-making power, but also introduces new challenges.

The large-scale volume of transactions in P2P energy trading imposes higher demands on computational efficiency [4]. To meet the demands of extensive trading, developing optimization algorithms with low computational complexity becomes crucial. In the context of the

coupling between carbon emissions and electricity, the distribution of benefits among different participants becomes increasingly complex. This not only requires the design of efficient trading mechanisms to incentivize bilateral transactions, but also necessitates the fair allocation of benefits from both carbon and energy trading, while carefully considering agent behaviors.

The diverse trading attributes in P2P energy trading, including large volumes of sensitive information such as agents' energy demand, supply capacity, and transaction prices, inevitably raise concerns regarding the exposure of private agent data. As a result, ensuring privacy protection without compromising transaction efficiency and flexibility has become a critical research challenge in the field of P2P energy trading [5]. Furthermore, P2P energy trading facilitates the integration of renewable energy by enabling flexible trading mechanisms. However, as the penetration of renewable energy increases, its output, which is heavily influenced by weather conditions, exhibits significant uncertainty and intermittency, thereby complicating modeling and increasing computational burdens.

* Corresponding authors.

E-mail addresses: zhanglu1@cau.edu.cn (L. Zhang), Jin.Yang@glasgow.ac.uk (J. Yang).

<https://doi.org/10.1016/j.apenergy.2025.125409>

Received 7 October 2024; Received in revised form 6 January 2025; Accepted 20 January 2025

Available online 4 February 2025

0306-2619/© 2025 The Authors. Published by Elsevier Ltd. This is an open access article under the CC BY license (<http://creativecommons.org/licenses/by/4.0/>).

Nomenclature**Indices**

(i, j)	Indices of beginning/ending buses of one branch
$[j]$	Variable for Local j th atomic copies
h, i, j	Indices of buses in the distribution system
n	Indices of scenarios
t	Indices of time points

Sets

B	Set of all branches in the distribution system
I	Set of terminal buses which directly connect with the agents in the distribution system and $I = \{1, \dots, I \}$
K	Set of all downstream buses and upstream buses which connect with the same beginning bus j
N	Set of scenarios and $N = \{1, \dots, N \}$
T	Set of time points and $T = \{1, \dots, T \}$

Variables

$\lambda_{jh,t}^{p2p}$	P2P electricity trading price between agents j and h at time t
μ_{jh}^{p2p}	P2P carbon quota trading price between agents j and h
μ_j	Lagrange multipliers with local constraints for agent j
ν_j	Lagrange multipliers with coordinated constraints for agent j
ω_j	Comprehensive contribution factor for agent j
ω_j^P	Electricity contribution factor for agent j
ω_j^R	Carbon contribution factor for agent j
A_j	Operational cost for agent j
a_j	Atomization variables of agent j
B_j	P2P trading cost for agent j
C_j^{p2p}	P2P electricity trading cost for agent j
C_j^{ESS}	ESS battery degradation cost for agent j
C_j^{DR}	DR compensation cost for agent j
C_j^{MT}	MT electricity generation cost for agent j
$C_j^{utility}$	Transaction cost with utilities for agent j
D_j	Total cost for agent j
D_j^0	Cost without participating in P2P energy trading for agent j
E_j^{p2p}	P2P carbon quota trading cost for agent j
E_j^{cet}	Carbon market trading cost for agent j
$I_{ij,t}$	Current for distribution branch (i, j) at time t
$l_{ij,t}$	Squared current for distribution branch (i, j) at time t

$P_{ij,t}$	Active power flowing of the branch (i, j) at time t
$P_{j,t}$	Active power at bus j at time t
$P_{j,t}^{ESS}$	Net power from ESS of agent j at time t
$P_{j,t}^{ch}$	Charge power from ESS of agent j at time t
$P_{j,t}^{dch}$	Discharge power from ESS of agent j at time t
$P_{j,t}^{DR,dn}$	Downward DR power for agent j at time t
$P_{j,t}^{DR,up}$	Upward DR power for agent j at time t
$P_{j,t}^{DR}$	Net DR power of agent j at time t
$P_{j,t}^{utility}$	Active Power traded with the utility by agent j at time t
$P_{j,t}^d$	Demand power of agent j at time t
$P_{j,t}^{MT}$	Active power output from MT of agent j at time t
$P_{j,t}^{PV,fcast}$	Forecasted power output from PV of agent j at time t
$P_{j,t}^{PV}$	Power output from PV of agent j at time t
$P_{j,t}^{WT,fcast}$	Forecasted power output from WT of agent j at time t
$P_{j,t}^{WT}$	Power output from WT of agent j at time t
$P_{jh,t}^{p2p}$	P2P active power transaction between agents j and h at time t
P_j^{rec}	Total Active power received by agent j during an operational cycle
P_j^{sup}	Total Active power supplied by agent j during an operational cycle
$Q_{ij,t}$	Reactive power flowing of the branch (i, j) at time t
$Q_{j,t}$	Reactive power at bus j at time t
$Q_{j,t}^{DR}$	Reactive power from DR of agent j at time t
$Q_{j,t}^d$	Reactive power demand of agent j at time t
$Q_{j,t}^{PV}$	Reactive power output from PV of agent j at time t
$Q_{j,t}^{WT}$	Reactive power output from WT of agent j at time t
$Q_{j,t}^{MT}$	Reactive power output from MT of agent j at time t
$Q_{j,t}^{PV}$	Reactive power output from PV of agent j at time t
r	Solar irradiance
R^{sum}	Total carbon quota of Cooperative Alliance during an operational cycle
R_{jh}^{p2p}	P2P carbon quota transaction between agents j and h at time t
R_j	Marginal contribution of agent j
R_j^{cet}	Carbon emission trading amount for agent j
R_j^{sum}	The total carbon quota of the alliance when agent j not participate in P2P energy trading
$SoC_{j,t}$	State of Charge of ESS for agent j at time t

To address these challenges, P2P energy trading should balance market mechanism design, privacy protection, and uncertainty modeling. Game-theoretic approaches to market design ensure fair benefits for all participants, while distributed algorithms provide privacy protection and enhance computational efficiency to accommodate the high frequency and volume of P2P transactions. Additionally,

optimizing the modeling of renewable energy uncertainty is essential. These complexities necessitate research that not only improves trading efficiency but also accounts for the variability of renewable energy outputs and the security of transaction data, thereby ensuring model robustness, practical applicability, and equitable distribution of benefits.

$SoC_{j,t}^{aux}$	Auxiliary State of Charge of ESS for agent j at time t
$U_{j,t}$	Magnitude voltage for bus j at time t
v	Wind speed
$V_{j,t}$	Magnitude of squared voltage for bus j at time t
y	The decision vectors of all agents in the distribution system
Parameters	
α	Distributionally robust reliability level
α^*	PDF confidence
η^{ch}	Charge efficiency of ESS
η^{dch}	Discharge efficiency of ESS
ρ	PAC algorithm parameters
t	Shape parameter affecting the left tail of the Beta distribution
κ	The benchmark price of carbon quota
λ_{net}	P2P network usage fee
c^{ESS}	Cost coefficient for ESS battery degradation
c^{DR}	Cost coefficient for DR compensation
c^{MT}	Cost coefficient for MT generation electricity
e^{GT}	Carbon emission factor for MT power
$e^{utility}$	Carbon emission factor for utility power
$\overline{I_{ij}}$	Maximum current limit on branch ij
$\overline{P_{j,t}^{DR}}$	Upper limit of DR power for agent j at time t
$\overline{P_j^{ch}}$	Maximum charge power from ESS of agent j
$\overline{P_j^{dch}}$	Maximum discharge power from ESS of agent j
$\overline{P_j^{MT}}$	Upper limit of active power output from MT of agent j
$\overline{Q_j^{MT}}$	Upper limit of reactive power output from MT of agent j
$\overline{Q_j^{PV}}$	Upper limit of reactive power from PV of agent j
$\overline{Q_j^{WT}}$	Upper limit of reactive power from WT of agent j
$\overline{SoC_j}$	Maximum State of Charge limit of ESS for agent j
$\overline{U_j}$	Maximum voltage magnitude limit at bus j
$\overline{\lambda_t^{P2P}}$	Upper bound for P2P electricity trading prices
$\overline{\mu^{P2P}}$	Upper bound for P2P carbon quota trading prices
γ_j	PAC algorithm parameters
ϑ	PAC algorithm time-variant factors
$\overline{I_{ij}}$	Minimum current limit on branch ij
$\overline{P_{j,t}^{DR}}$	Lower limit of DR power for agent j at time t

$\underline{P_j^{MT}}$	Lower limit of active power output from MT of agent j
$\underline{Q_j^{MT}}$	Lower limit of reactive power output from MT of agent j
$\underline{Q_j^{PV}}$	Lower limit of reactive power from PV of agent j
$\underline{Q_j^{WT}}$	Lower limit of reactive power from WT of agent j
$\underline{SoC_j}$	Minimum State of Charge limit of ESS for agent j
$\underline{U_j}$	Minimum voltage magnitude limit at bus j
$\underline{\lambda_t^{P2P}}$	Lower bound for P2P electricity trading prices
$\underline{\mu^{P2P}}$	Lower bound for P2P carbon quota trading prices
θ	PAC algorithm time-variant factors
φ^{DR}	Power factor for DR
φ_j^{MT}	Power factor for MT j
ζ	Shape parameter affecting the right tail of the distribution
ε	PAC algorithm time-variant factors
ξ	The growth rate
B	Matrix of coefficients for the coordination constraints
b	Vector of constants for the equality constraints in the optimization problem
c	Scale parameter of the Weibull distribution
$c_t^{utility}$	Time-of-use electricity pricing from the utility
D	The pricing interval
d_{KL}	KL divergence
E_j^{ESS}	Energy capacity of ESS for agent j
G	Matrix of coefficients for the equality constraints in the optimization problem
k	Shape parameter of the Weibull distribution
$P_j^{PV, rated}$	Rated power output from PV of agent j
$P_j^{WT, rated}$	Rated power output from WT of agent j
r_{ij}	Resistance of the branch between bus i and j
RD_j	Ramp-down of MT for agent j
RU_j	Ramp-up of MT for agent j
$S_{j, end}$	Ending State of Charge of ESS for agent j
S_j^{PV}	Apparent power capacity from PV of agent j
S_j^{WT}	Apparent power capacity from WT of agent j
$SoC_{j, ini}$	Initial State of Charge of ESS for agent j
v_c	Cut-in wind speed
v_o	Cut-out wind speed
v_r	Rated wind speed
x_{ij}	Reactance of the branch between bus i and j
r_r	Rated solar irradiance level

1.2. Literature review

In the design of market mechanisms, game theory serves as a crucial theoretical foundation for modeling the interactions among participants in P2P energy trading markets. Studies [6,7] introduce a Stackelberg game framework within microgrids, where producers act

as leaders and consumers as followers, demonstrating that producers can achieve higher profits under this structure. Conversely, another line of research [8,9] examines the dynamics of non-cooperative games between producers and consumers, such as energy centers. However, P2P energy trading typically involves medium- to long-term contracts

and operates within markets characterized by limited competition. This environment renders cooperative game models more appropriate in practical applications [10]. For instance, one study [11] develops a cooperative game framework tailored for community microgrids, utilizing the Shapley value for revenue distribution. In contrast to the Shapley value allocation, this framework emphasizes Nash bargaining [12] as a cooperative game approach, which can more effectively balance the diverse objectives of different participants [13]. The Nash equilibrium is achieved in P2P trading scenarios when participants act rationally and the outcome is Pareto optimal. In [14], a cooperative scheduling framework based on the Nash bargaining model is proposed for P2P energy trading, involving both Distribution System Operators (DSOs) and consumers. This framework not only quantifies the impact of P2P electricity trading but also introduces an asymmetric Nash bargaining model for the distribution of profits between producers and consumers [15,16]. Beyond these considerations, it is essential for research to account for the effects of power transmission on the distribution network. Specifically, optimizing trading mechanisms to mitigate issues such as voltage violation and line capacity overloads is critical [17]. These factors represent significant challenges that must be addressed to ensure the practical viability and reliability of P2P energy trading systems.

Building upon the aforementioned market mechanisms and game-theoretic frameworks, traditional optimization methods typically require centralized processing within a dispatch control center. This centralized approach can demand significant computational resources, raise privacy concerns, and be susceptible to communication disruptions [18]. Specifically, centralized optimization techniques struggle to meet the demands of P2P energy trading, particularly when managing a large number of distributed energy resources and handling extensive datasets. To address these challenges, distributed algorithms have emerged as a promising solution for decentralized P2P energy markets. Methods such as the dual ascent method [19] and the primal-dual method [20] are well-established approaches in this domain. Notably, the Alternating Direction Method of Multipliers (ADMM) [21] integrates the strengths of primal-dual techniques and augmented Lagrangian methods, offering stable convergence properties, ease of implementation, and broad applicability in P2P energy trading research. Leveraging the ADMM algorithm, recent studies have developed control architectures for P2P energy trading within multi-microgrid systems [22]. Additionally, ADMM has been utilized to optimize power flows in bilateral trading mechanisms within distribution networks, thereby enhancing economic efficiency [23]. Further contributions to the field include the development of various ADMM algorithm variants tailored to the specific requirements of P2P energy trading scenarios [24–26]. These advancements in distributed optimization not only complement the game-theoretic approaches previously discussed but also provide practical methodologies for implementing efficient P2P energy trading systems. By decentralizing the optimization process, these algorithms help mitigate the computational and privacy issues inherent in centralized methods, while also enhancing the overall stability and scalability of P2P energy markets.

Despite the numerous advantages of the ADMM algorithm, it also presents certain drawbacks, including privacy protection concerns and high computational complexity. To address these limitations, Romvay et al. [27] proposed the Proximal Atomic Coordination (PAC) algorithm, which is grounded in the primal-dual methodology and offers a unified framework for distributed convex optimization. The PAC algorithm is characterized by its rapid convergence and enhanced privacy protection capabilities. Its successful application in retail electricity markets has facilitated the compensation of distributed node marginal prices and enabled efficient energy scheduling [28]. However, there is an urgent need for further research on the application of the PAC algorithm within P2P energy trading contexts. Specifically, improvements in convergence efficiency and the development of algorithmic frameworks that ensure privacy protection are essential. This area

remains largely unexplored, presenting significant opportunities for advancing the state of distributed optimization in P2P energy markets.

Following the discussion of distributed optimization algorithms, it is also crucial to tackle the uncertainties present in P2P energy trading. Stochastic Programming (SP) [29], Robust Optimization (RO) [30], and Distributionally Robust Optimization (DRO) [31] have emerged as the most commonly employed methodologies in recent years. For example, the study by [32] integrates chance constraints with SP within a community market framework to ensure that reserve requirements are adequately satisfied. Similarly, another investigation [33] addresses uncertainties in P2P energy trading for integrated energy hubs by combining Conditional Value-at-Risk (CVaR) with SP. Wei et al. [34] utilize RO to mitigate the uncertainties associated with renewable energy sources, proposing a microgrid P2P energy trading framework that enhances both system adaptability and transaction stability. Building on this foundation, subsequent research [35] develops a two-layer robust optimization model to manage energy sharing in microgrids under uncertain conditions. Additionally, the study [36] explores the application of fuzzy sets based on deep Gaussian processes in conjunction with DRO to effectively handle uncertainties in P2P trading scenarios.

Despite the advantages of above methodologies, they each encounter significant challenges. SP requires extensive probabilistic data, which is often difficult to obtain in practice, and its outcomes can be overly optimistic [37]. RO, while providing robustness, tends to be overly conservative as it focuses on solutions for the worst-case scenarios. DRO combines the strengths of both SP and RO by utilizing historical data to achieve a balance between economic efficiency and robustness. Among DRO approaches, those based on Wasserstein metric have garnered considerable attention due to their superior traceability and out-of-sample performance [38,39]. However, Wasserstein-based DRO typically assumes a linear mapping between decision variables and uncertain parameters. In reality, the relationship between these variables may be nonlinear [40]. As a result, Wasserstein-based DRO with linear decision rules can produce suboptimal or even inaccurate results and may suffer from poor computational performance [41]. Furthermore, Wasserstein metric-based methods are highly dependent on the size of the sample data. When the sample size is small, there is a risk of overfitting [42], whereas excessively large sample sizes can lead to significant computational burdens [43]. These limitations highlight the need for continued research to enhance the efficiency and accuracy of DRO approaches in P2P energy trading contexts.

In parallel, another approach based on Kullback–Leibler (KL) divergence has also seen widespread application in recent years. For example, the study by [44] introduces a low-carbon optimization model for energy hubs and employs the Column-and-Constraint Generation (C&CG) algorithm to solve the DRO problem. However, the C&CG algorithm requires the introduction of new constraints in each iteration, which can significantly reduce computational efficiency in large-scale P2P energy trading scenarios [45]. Another investigation [46] transforms the KL divergence-based DRO model for community energy sharing into a mixed-integer linear programming (MILP) problem, enabling direct solution via standard solvers. Nonetheless, the inclusion of integer variables during this transformation renders the problem non-convex, thereby complicating the application of distributed algorithms and potentially undermining convergence guarantees [47]. Additionally, the study [48] proposes a KL divergence-based method for planning energy storage capacity. However, this approach has not been extended to distributed optimization frameworks suitable for P2P trading.

1.3. Research gap

Table 1 provides a comprehensive comparison of the selected studies presented in the Literature Review, focusing on aspects such as

uncertainty models, market mechanisms, network constraints, and distributed algorithms. Despite these efforts, existing research still exhibits several shortcomings in addressing P2P trading issues characterized by a large number of transactions, diverse types, and privacy protection requirements.

Firstly, in the realm of P2P market mechanisms, current studies are predominantly focused on the distribution of economic benefits, while neglecting critical factors such as carbon emission quota markets, the construction of trading mechanisms, and their environmental impacts. This oversight results in insufficient attention to the vital role of carbon trading in reducing greenhouse gas emissions and promoting sustainable development. Consequently, asymmetric Nash bargaining models in cooperative games, which are primarily driven by economic benefits, fail to adequately account for the effects of carbon quota trading.

Secondly, although distributed optimization algorithms exhibit promising applications in fully decentralized P2P energy trading, existing research predominantly focuses on enhancing the performance of the ADMM algorithm. There is a lack of systematic exploration into privacy protection characteristics within P2P trading frameworks. Specifically, when considering both market trading mechanisms and renewable energy uncertainties, significant research gaps persist. Therefore, the development and application of more general and efficient privacy-preserving distributed algorithms in P2P energy trading represent critical areas for current and future research efforts.

Lastly, concerning the uncertainty associated with renewable energy sources, DRO demonstrates potential in balancing economic efficiency and robustness. However, existing DRO methods based on Wasserstein metric and KL divergence suffer from significant limitations, including strong dependence on sample data, non-convex problem formulations, and high computational complexity. Moreover, applying DRO models to P2P energy trading presents challenges in developing efficient solving algorithms suitable for large-scale scenarios with uncertainty consideration. There remains a substantial research gap in achieving a balance between optimization performance and computational efficiency, ensuring distributed convergence, and addressing the unique uncertainty management challenges inherent in decentralized markets.

1.4. Contributions of this paper

To address the identified research gaps, this study introduces a novel P2P trading framework that first employs an asymmetric Nash bargaining framework to integrate the dynamics of carbon emission trading, ensuring fair revenue distribution and addressing cost allocation challenges in both P2P electricity and carbon quota markets. Next, the framework incorporates power flow constraints and utilizes an enhanced PAC algorithm to achieve a fully decentralized solution, guaranteeing privacy protection and computational efficiency in P2P energy trading. Finally, by leveraging KL divergence to construct probability distribution measures and applying convex and sample average approximation methods, the DRO problem is transformed into a Distributionally Robust Chance-Constrained (DRCC) problem. This transformation maintains the convexity of the modeling framework and effectively manages the inherent uncertainties of renewable energy sources. In summary, the primary contributions of this paper are as follows:

- **Integration of Network Constraints and Asymmetric Nash Bargaining:** This study introduces the asymmetric Nash bargaining theory to determine P2P trading prices under the network constraints. It proposes a marginal effect contribution of carbon quotas and nonlinear mappings of the contribution factors from both electricity and carbon quota transactions. This approach maximizes each agent's benefits while promoting efficient energy trading. The comprehensive consideration of electrical and carbon emission trades ensures fair cost and revenue distribution among agents.

- **Development of a Decentralized P2P Energy Trading Framework with Enhanced Privacy:** A decentralized P2P energy trading framework is developed to significantly improve transaction privacy. This framework employs time-varying factors to obscure the true values of transfer variables in each iteration, effectively preventing their recovery. Comparative analyses with the widely used ADMM algorithm in current P2P energy trading demonstrate the superior convergence speed, computational efficiency, and privacy protection offered by the PAC algorithm. This framework provides an efficient and privacy-preserving solution for P2P energy trading, thereby supporting the practical implementation of decentralized trading systems.
- **Application of Data-Driven DRCC Methods for P2P Energy Trading:** To address the uncertainty associated with renewable energy generation installed by agents, a data-driven DRCC approach is adopted. By introducing KL divergence-based probability distribution sets into the distributed optimization model, this method maintains the convexity of the model, ensuring its compatibility with P2P distributed trading frameworks and guaranteeing algorithmic convergence. This significantly enhances the adaptability and stability of the model in large-scale and complex trading environments characterized by uncertainty.

In summary, this paper makes significant advancements by integrating DRO techniques with game-theoretic approaches and decentralized algorithms, thereby addressing critical challenges in P2P energy trading. The proposed framework not only ensures fair and efficient energy and carbon trading but also enhances privacy and computational efficiency, making it a robust solution for modern decentralized energy markets.

2. Preliminaries

2.1. Overview

The main outline (shown in Fig. 1) of this paper is as follows: Section 3 focuses on the construction of uncertainty sets for wind speed and solar radiation intensity, as well as the modeling of controllable devices within distribution systems. The construction of uncertainty sets is crucial for predicting and optimizing renewable energy systems, while the precise modeling of controllable devices provides the necessary foundation for subsequent trading mechanism formulation and system optimization. Section 4 constructs a trading mechanism under a cooperative alliance, aiming to achieve effective resource allocation, minimization of cooperative alliance costs, and fair distribution of benefits through collaborative efforts among agents. Section 5 introduces the PAC algorithm and explores its application in the research problem model presented in this study. The PAC algorithm, as an efficient and privacy-protected distributed algorithm, has significant advantages in handling large-scale P2P energy trading issues. Section 6 validates the effectiveness of the proposed models and algorithms through case studies. Section 7 summarizes the entire paper and reviews the main contributions of the research.

2.2. Research assumptions

In this study, several assumptions and simplifications have been employed. These are summarized as follows:

- Each agent is able to engage in transactions of any volume with all other agents participating in the P2P energy trading network.
- The agents are located in a close position to each other, and the wind speed or solar radiation intensity within the distribution system is assumed to follow the same distribution.
- The P2P energy trading between agents involves both electricity and carbon quotas, with the electricity trading focusing on active power.

Table 1
Comparison of the proposed technique with existing P2P literature.

Reference	Uncertainty model	Probability distribution measurement	Market mechanism	Network constraints	Model	Distributed algorithm	Communication variable protection
[34]	RO	×	Nash bargaining	×	Convex	ADMM	×
[39]	DRO	Wasserstein metric	×	✓	Convex	ADMM	×
[32]	Chance-constrained	×	×	×	Convex	ADMM	×
[33]	CVAR-SP	×	Nash bargaining	✓	Convex	×	×
[7]	×	×	Stackelberg game	✓	MISOCP	×	×
[9]	×	×	Non-cooperative game	×	MILP	×	×
[12]	×	×	Nash bargaining	✓	Convex	ADMM	×
[14]	×	×	Nash bargaining	✓	Convex	ADMM	×
[16]	CVAR-SP	×	Asymmetric nash bargaining	×	MILP	×	×
[24]	×	×	×	✓	Convex	R-ADMM	×
[25]	×	×	×	✓	Convex	F-ADMM	×
[26]	×	×	Asymmetric nash bargaining	×	Convex	WAS-ADMM	×
[49]	×	×	×	✓	Convex	ADMM	×
This paper	DRCC	KL divergence	Asymmetric nash bargaining	✓	Convex	PAC	✓

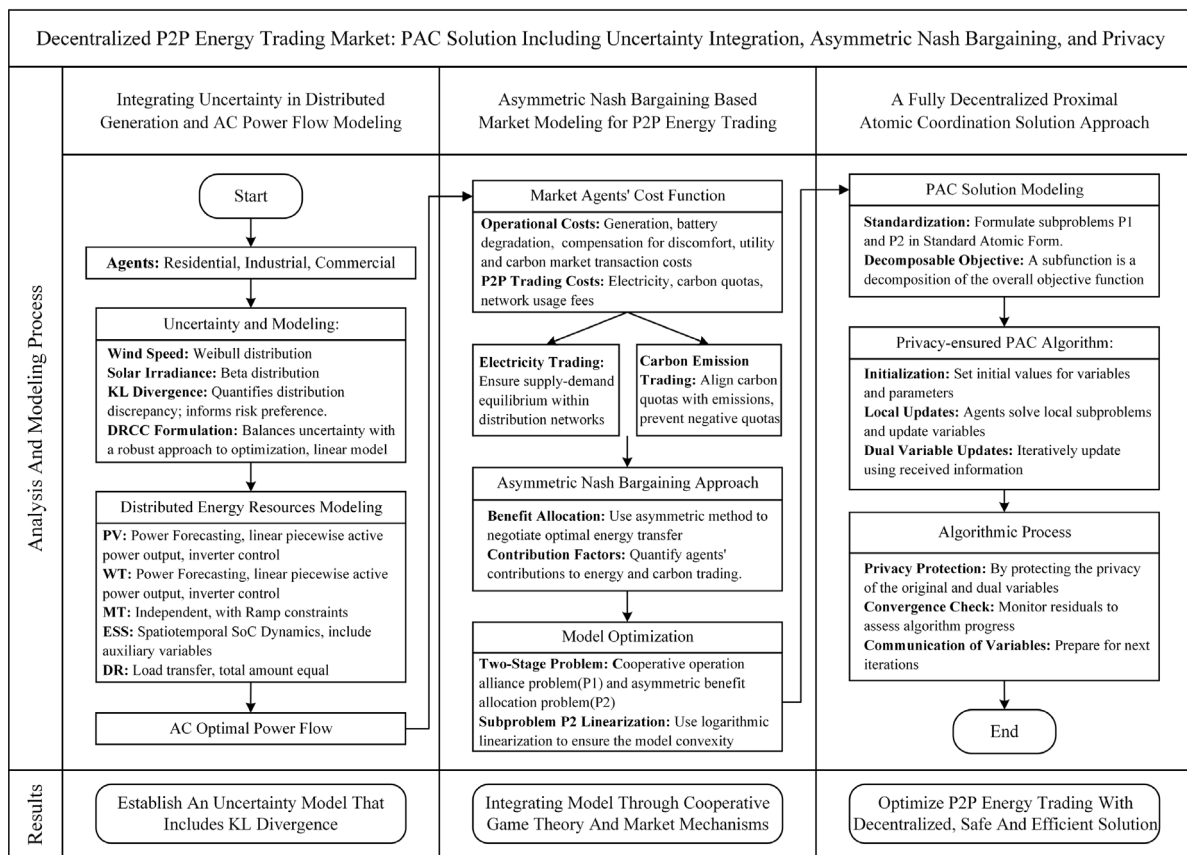


Fig. 1. The main outline of this article.

- Active power losses due to distribution are the responsibility of the electricity seller and are paid to DSOs.
- All agents are assumed to be rational, striving to maximize both their individual benefits and the collective interests of the cooperative alliance.

3. Uncertainty and distributed resource modeling in distribution system

Energy prosumers, who are equipped with energy resources such as wind turbines(WT), photovoltaic panels(PV), micro gas turbines(MT), and energy storage systems (ESS), have the potential to generate a

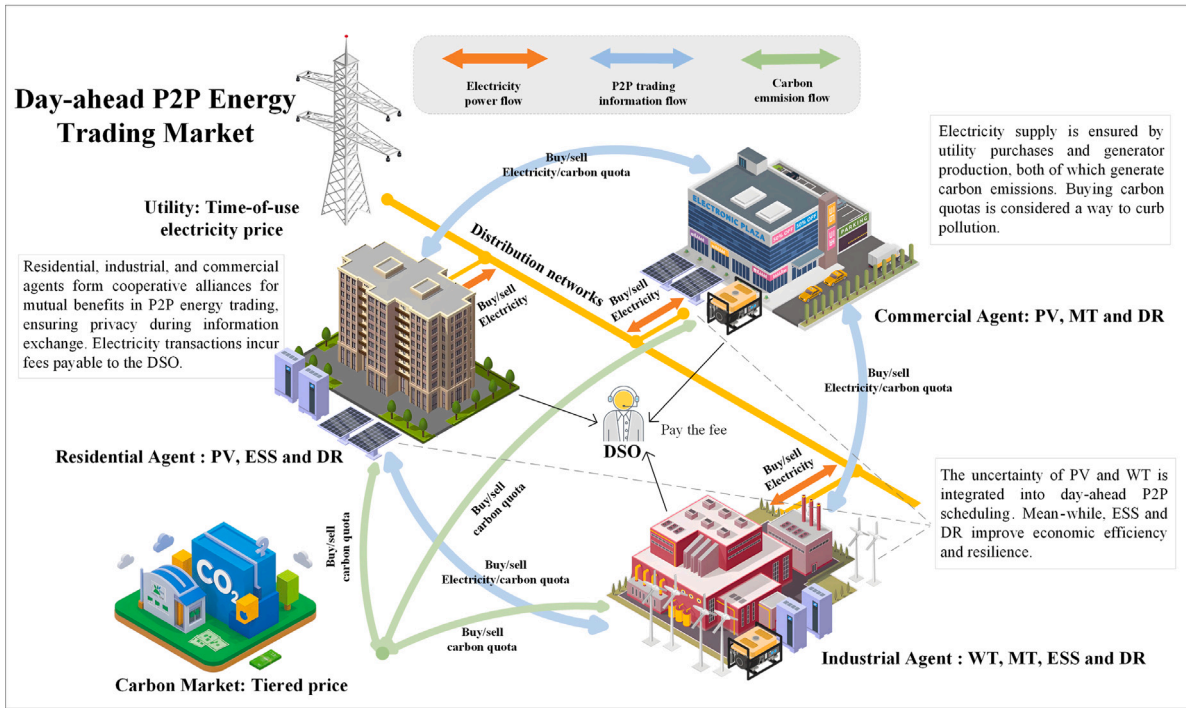


Fig. 2. Diagram of P2P energy trading market.

surplus of energy that exceeds their own consumption. In addition, demand response (DR) can be viewed as a special kind of energy resource because it involves adjusting electricity consumption in response to changes in utility conditions or electricity prices. Their flexibility positions them as active participants in the day-ahead P2P energy market, where each participant acts as an agent. The day-ahead P2P energy trading market architecture mentioned in this article is shown in Fig. 2.

3.1. Renewable energy resources output modeling

The generation of energy from WT and PV is subject to significant fluctuations depending on weather conditions, which can have a considerable impact on the outcomes of P2P energy trading. The probabilistic analysis and power output modeling of these renewable energy sources are presented in [50,51]. Relevant derivations in this section, including the SP and RO models, can be found in Appendix A.

3.1.1. Uncertainty set modeling based on KL divergence

To address the uncertainty in the output of renewable energy sources for agents, this article uses the KL divergence to express the distance between different probability distribution functions, denoted D_{KL} . The smaller the value of D_{KL} is, the closer the two distribution functions are to each other. For a continuous actual probability density function f and a reference probability density function f_0 , the KL divergence D_{KL} is defined as follows:

$$D_{KL}(P \parallel P_0) = \int_{\Omega} f(\xi) \ln f(\xi) / f_0(\xi) d\xi \quad (1)$$

For discrete probability density functions f and the reference probability density function f_0 , the D_{KL} is defined as follows:

$$D_{KL}(P \parallel P_0) = \sum_n \pi_n \ln f(\pi_n) / f_0(\pi_n^0) \quad \forall n \quad (2)$$

This paper considers all distribution functions that have a distance from the empirical probability density function not exceeding the maximum tolerance value d_{KL} . An uncertain set of distribution functions is

established as follows:

$$\sigma = \{f \mid D_{KL}(f \parallel f_0) \leq d_{KL}\} \quad (3)$$

Here the d_{KL} selection mirrors an agent's risk preference, with lower values indicating tighter alignment with renewable energy's actual distribution and higher values suggesting greater divergence. To achieve equilibrium in risk aversion, the determination of d_{KL} is defined as follows:

$$d_{KL} = \frac{1}{2N} \chi_{N-1, \alpha^*}^2 \quad (4)$$

When the problem is characterized using KL divergence, as referenced in [52], The confidence selection in the DRCC is given by the following formula:

$$\alpha_+ = \max \left\{ 0, 1 - \inf_{z \in (0,1)} \left\{ \frac{e^{-d_{KL} z^{1-\alpha}} - 1}{z - 1} \right\} \right\} \quad (5)$$

where determination of the α_+ can be achieved using the bisection method, as discussed in [53].

3.1.2. Wind turbines

The probability density function (PDF) of wind speed is described by a two-parameter Weibull distribution, which is utilized for forecasting the probability distribution of wind speeds, calibrated to historical wind speed data:

$$f(v) = \frac{k}{c} \left(\frac{v}{c}\right)^{k-1} \exp\left[-\left(\frac{v}{c}\right)^k\right] \quad (6)$$

The power output of a WT is modeled concisely as follows:

$$P_{j,t,n}^{WT,fcst} = \begin{cases} 0 & v_n(t) < v_c, v_n(t) \geq v_o \\ P_j^{WT,rated} \frac{(v_n(t)-v_c)}{v_r-v_c} & v_c \leq v_n(t) < v_r \\ P_j^{WT,rated} & v_r \leq v_n(t) < v_o \end{cases} \quad \forall j \in I, \forall t, \forall n \quad (7)$$

$$P_{j,t}^{WT} - P_{j,t,n}^{WT,fcst} + \beta_{j,t} \leq \phi_{j,n}, \quad \phi_{j,n,t} \geq 0 \quad \forall j \in I, \forall t, \forall n \quad (8)$$

$$\sum_n \pi_{j,n} \phi_{j,n,t} \leq \beta_{j,t} \alpha_+, \quad \beta_{j,t} > 0 \quad \forall j \in I, \forall t, \forall n \quad (9)$$

$$\underline{Q_j^{WT}} \leq Q_{j,t}^{WT} \leq \overline{Q_j^{WT}} \quad \forall j \in I, \forall t \quad (10)$$

$$|Q_{j,t}^{WT}| \leq \sqrt{(S_j^{WT})^2 - (P_{j,t}^{WT})^2} \quad \forall j \in I, \forall t \quad (11)$$

where the WT's forecasting active power, as depicted in Eq. (7), is mainly dependent on the wind speed, manifesting in a piecewise function form. Power generation is inactive above the cut-out or below the start-up wind speeds. A linear increase in maximum output power is observed between the start-up and rated wind speeds. The turbine's maximum output power reaches its rated capacity at wind speeds above the rated but below the cut-out speed. Eqs. (8), (9) calculates the probability that the actual WT output power is less than the power generation possible under a distribution with Weibull standard deviation. Eq. (10) regulates the reactive power output of the WT, while Eq. (11) ensures that the turbine's active and reactive power meet the apparent power constraints.

3.1.3. Photovoltaic panels

The PDF of the solar irradiance follows a Beta distribution:

$$f(r) = \frac{\Gamma(t + \zeta)}{\Gamma(t)\Gamma(\zeta)} (r)^{t-1} (1-r)^{\zeta-1} \quad (12)$$

where the shape parameters t and ζ indicate the behavior of the Beta distribution's tails. Estimating these parameters from historical irradiance data enables the prediction of the solar irradiance probability distribution.

PV power generation is modeled to represent the conversion of solar energy into electrical power.

$$P_{j,t,n}^{PV,fcst} = \begin{cases} P_j^{PV,rated} \frac{r_n(t)}{r_r} & 0 \leq r_n(t) < r_r \\ P_j^{PV,rated} & r_r \leq r_n(t) \end{cases} \quad \forall j \in I, \forall t, \forall n \quad (13)$$

$$P_{j,t}^{PV} - P_{j,t,n}^{PV,fcst} + \beta_{j,t} \leq \phi_{j,n,t}, \quad \phi_{j,n,t} \geq 0 \quad \forall j \in I, \forall t, \forall n \quad (14)$$

$$\sum_n \pi_{j,n} \phi_{j,n,t} \leq \beta_{j,t} \alpha_+, \quad \beta_{j,t} > 0 \quad \forall j \in I, \forall t, \forall n \quad (15)$$

$$\underline{Q_j^{PV}} \leq Q_{j,t}^{PV} \leq \overline{Q_j^{PV}} \quad \forall j \in I, \forall t \quad (16)$$

$$|Q_{j,t}^{PV}| \leq \sqrt{(S_j^{PV})^2 - (P_{j,t}^{PV})^2} \quad \forall j \in I, \forall t \quad (17)$$

where PV output power, as per Eq. (13), is mainly dependent on solar irradiance and shows linear characteristics of a linear function in active power output. Eqs. (14), (15) calculate the probability of the actual PV output power when it is less than the power generation possible under a distribution with Beta standard deviation. Eq. (16) shows the reactive power limits of PV generation. Eq. (17) indicates that the PV system, via an inverter, keeps the active and reactive power within the maximum apparent power constraints.

3.2. Micro gas turbines

MTs supply extra power to agents, unaffected by renewable energy outputs. The modeling of these devices in this paper is based on [54]:

$$\underline{P_j^{MT}} \leq P_{j,t}^{MT} \leq \overline{P_j^{MT}} \quad \forall j \in I, \forall t \quad (18)$$

$$\underline{Q_j^{MT}} \leq Q_{j,t}^{MT} \leq \overline{Q_j^{MT}} \quad \forall j \in I, \forall t \quad (19)$$

$$RD_j \leq P_{j,t+1}^{MT} - P_{j,t}^{MT} \leq RU_j \quad \forall j \in I, \forall t \quad (20)$$

$$\tan(\arccos(-\phi_j^{MT})) \leq Q_{j,t}^{MT} / P_{j,t}^{MT} \leq \tan(\arccos(\phi_j^{MT})) \quad \forall j \in I, \forall t \quad (21)$$

where the operational constraints on the output power of an MT are delineated by Eqs. (18) and (19). Eq. (20) specifies the ramping characteristics of the turbine. The reactive power output properties of MTs are captured in Eq. (21).

3.3. Energy storage systems

ESS should be modeled with consideration of spatiotemporal coupling. Proper utilization of ESS not only allows for the flexible adjustment of electricity loads to meet varying energy needs at different times but also optimizes cost-effectiveness through the strategic use of time-variant electricity pricing, as discussed in [55].

$$P_{j,t}^{ESS} = P_{j,t}^{dch} - P_{j,t}^{ch} \quad \forall j \in I, \forall t \quad (22)$$

$$0 \leq P_{j,t}^{dch} \leq \overline{P_j^{dch}} \quad \forall j \in I, \forall t \quad (23)$$

$$0 \leq P_{j,t}^{ch} \leq \overline{P_j^{ch}} \quad \forall j \in I, \forall t \quad (24)$$

$$\underline{SoC_j} \leq SoC_{j,t} \leq \overline{SoC_j} \quad \forall j \in I, \forall t \quad (25)$$

$$SoC_{j,ini} = SoC_{j,end} \quad \forall j \in I \quad (26)$$

$$SoC_{j,t+1} = SoC_{j,t} + (\eta^{ch} P_{j,t}^{ch} - P_{j,t}^{dch} / \eta^{dch}) / E_j^{ESS} \quad \forall j \in I, \forall t \quad (27)$$

$$SoC_{j,t+1}^{aux} = SoC_{j,t} - P_{j,t}^{dch} / \eta^{dch} / E_j^{ESS} \quad \forall j \in I, \forall t \quad (28)$$

where the constraints on the ESSs' charge and discharge power and its State of Charge (SOC) are defined by Eqs. (22), (23) and (25). The SOC of the ESS at any given time is determined using Eq. (27). An auxiliary cost calculation for the ESS is facilitated by the introduction of Eq. (28). Eq. (26) ensures the SOC of the ESS is identical at the start and end of each cycle.

3.4. Demand response

At each agent node, DR constraints include the sum of non-flexible and flexible loads, with non-flexible loads being essential and uninterruptible. Agents can participate in DR by adjusting strategies for flexible loads, such as production schedules or air conditioning systems. Exceeding or falling short of the load demand can impact agent comfort, potentially incurring discomfort costs, for which appropriate compensation is pursued.

$$P_{j,t}^{DR} = P_{j,t}^{DR,dn} - P_{j,t}^{DR,up} \quad \forall j \in I, \forall t \quad (29)$$

$$\underline{P_{j,t}^{DR}} \leq P_{j,t}^{DR} \leq \overline{P_{j,t}^{DR}} \quad \forall j \in I, \forall t \quad (30)$$

$$\sum_t P_{j,t}^{DR,up} = \sum_t P_{j,t}^{DR,dn} \quad \forall j \in I, \forall t \quad (31)$$

$$Q_{j,t}^{DR} = P_{j,t}^{DR} \tan(\arccos(\phi^{DR})) \quad \forall j \in I, \forall t \quad (32)$$

where the constraints on the load shifting that impact agent comfort at any given instant are defined by Eq. (30), which sets the upper and lower bounds for such shifts. Eq. (31) maintains the equality of total load before and after the shifting process. Eq. (32) relates the shifted active power to the transferred reactive power load.

3.5. AC power flow model

This paper evaluates the impact of P2P energy trading on distribution lines and ensures transaction feasibility using a second-order cone relaxation-based AC power flow model, as referenced in [56]:

$$P_{j,t} = \sum_{i \in K} (P_{ij,t} - l_{ij,t} r_{ij}) - \sum_{k \in K} P_{jk,t} \quad \forall (i, j, k) \in B, \forall t \quad (33)$$

$$Q_{j,t} = \sum_{i \in K} (Q_{ij,t} - l_{ij,t} x_{ij}) - \sum_{k \in K} Q_{jk,t} \quad \forall (i, j, k) \in B, \forall t \quad (34)$$

$$P_{j,t} = -P_{j,t}^{\text{utility}} - \sum_h P_{jh,t}^{\text{P2P}} \quad \forall h \in I/j, \forall j \in I, \forall t \quad (35)$$

$$Q_{j,t} = -Q_{j,t}^{\text{d}} + Q_{j,t}^{\text{MT}} + Q_{j,t}^{\text{WT}} + Q_{j,t}^{\text{PV}} + Q_{j,t}^{\text{DR}} \quad \forall j \in I, \forall t \quad (36)$$

$$V_{j,t} = V_{i,t} - 2(r_{ij} P_{ij,t} + x_{ij} Q_{ij,t}) + (r_{ij}^2 + x_{ij}^2) l_{ij,t} \quad \forall (i, j) \in B, \forall t \quad (37)$$

$$\|2P_{ij,t} \quad 2Q_{ij,t} \quad l_{ij,t} - V_{i,t}\|_2 \leq l_{ij,t} + V_{i,t} \quad \forall (i, j) \in B, \forall t \quad (38)$$

$$\underline{U}_j \leq U_{j,t} \leq \overline{U}_j \quad \forall j \in B, \forall t \quad (39)$$

$$\underline{I}_{ij} \leq I_{ij,t} \leq \overline{I}_{ij} \quad \forall (i, j) \in B, \forall t \quad (40)$$

where the active power balance within the agent's distribution system, considering network losses, is encapsulated by Eq. (33). Eq. (34) delineates the sources of reactive power, namely MT, WT and PV systems, which are integral to maintaining distribution system stability. To ensure the stability and reliability of the distribution system, nodal voltage drops are governed by Eq. (37), with further regulation by Eq. (39) to keep the voltage within acceptable thresholds. The constraints post second-order cone relaxation are articulated by Eq. (38), refining the model for more accurate power flow analysis. Lastly, Eq. (40) imposes limits on the current, safeguarding the system from potential damage due to excessive current flow.

4. Nash bargaining based market modeling for P2P electricity and carbon emission trading

Building upon the analysis of uncertainties in distributed generation and AC power flow, this section delves into Nash bargaining-based market modeling for P2P energy trading. It defines the cost structures for market agents, encompassing both operational and trading expenses. Operational costs include those for MT generation, ESS degradation, DR compensation, and utility interactions, while P2P trading costs involve electricity volumes and carbon quotas. This section establishes constraints related to energy balance and carbon quotas and employs an asymmetric Nash bargaining approach to optimize benefit distribution among agents. This approach is framed as a two-stage problem, addressing both optimal energy transmission and pricing strategies within the P2P market.

4.1. Market agents' cost function

Here each agent's cost D_j structure includes operational costs A_j and P2P trading costs B_j .

$$D_j = A_j + B_j \quad \forall j \in I \quad (41)$$

Operational costs consist of MT electricity generation costs, ESS battery degradation costs, costs for DR compensation, and transaction costs with utilities and the tiered carbon pricing market [26].

$$A_j = \min(C_j^{\text{MT}} + C_j^{\text{ESS}} + C_j^{\text{DR}}) \quad \forall j \in I \quad (42)$$

$$C_j^{\text{MT}} = \sum_t c_t^{\text{MT}} P_{j,t}^{\text{MT}} \quad \forall j \in I, \forall t \quad (43)$$

$$C_j^{\text{ESS}} = \sum_{t=2} c_t^{\text{ESS}} (SoC_{j,t-1} - SoC_{j,t}^{\text{aux}}) \quad \forall j \in I, \forall t \quad (44)$$

$$C_j^{\text{DR}} = c^{\text{DR}} \sum_t (P_{j,t}^{\text{DR,up}} + P_{j,t}^{\text{DR,dn}}) \quad \forall j \in I, \forall t \quad (45)$$

$$C_j^{\text{utility}} = \sum_t c_t^{\text{utility}} P_{j,t}^{\text{utility}} \quad \forall j \in I, \forall t \quad (46)$$

$$E_j^{\text{cet}} = \begin{cases} \kappa R_j^{\text{cet}} & -D < R_j^{\text{cet}} \leq D \\ \kappa(1 + \xi)(R_j^{\text{cet}} - D) + \kappa D & D < R_j^{\text{cet}} \leq 2D \\ \kappa(1 + 2\xi)(R_j^{\text{cet}} - 2D) + \kappa(2 + \xi)D & 2D < R_j^{\text{cet}} \leq 3D \\ \kappa(1 + 3\xi)(R_j^{\text{cet}} - 3D) + \kappa(3 + \xi)D & 3D < R_j^{\text{cet}} \leq 4D \\ \dots & \dots \end{cases} \quad \forall j \in I \quad (47)$$

where the generation cost of MT is depicted using a linear function [57]. Similarly, the degradation cost of ESS is calculated through auxiliary variables, efficiently bypassing mixed-integer complexities in the cost estimation. In our approach, hourly transactions with utility companies are affected by the time-of-use pricing. In the meantime, daily carbon market transactions employ a tiered pricing system with a compensation coefficient to encourage emission reductions. This system is structured in a way that results in higher trading volumes leading to increased costs in the carbon market.

The cost of P2P energy trading encompasses the expenses associated with energy trading with other agents. This energy trading is divided into two components: electricity volumes and carbon quotas. These P2P energy trading serves to fulfill the agent's demands or generate profit. The modeling of this process is as follows.

$$B_j = C_j^{\text{P2P}} + E_j^{\text{P2P}} \quad \forall j \in I \quad (48)$$

$$C_j^{\text{P2P}} = \sum_t \sum_h (\lambda_{jh,t}^{\text{P2P}} P_{jh,t}^{\text{P2P}} + \lambda_{jh,t}^{\text{net}} \max\{P_{jh,t}^{\text{P2P}}, 0\}) \quad \forall h \in I/j, \forall j \in I, \forall t \quad (49)$$

$$E_j^{\text{P2P}} = \sum_h \mu_{jh}^{\text{P2P}} R_{jh}^{\text{P2P}} \quad \forall h \in I/j, \forall j \in I \quad (50)$$

where P2P energy sellers pay a network usage fee to the DSOs. The implementation of network usage fees represents a regulatory measure designed to prevent the exploitation of energy arbitrage in P2P energy trading.

Agents in the distribution system must fulfill both their intrinsic energy balance constraints and the equilibrium constraints of P2P energy trading.

$$P_{j,t}^{\text{utility}} + \sum_h P_{jh,t}^{\text{P2P}} = P_{j,t}^{\text{d}} - P_{j,t}^{\text{MT}} - P_{j,t}^{\text{WT}} - P_{j,t}^{\text{PV}} - P_{j,t}^{\text{ESS}} - P_{j,t}^{\text{DR}} \quad \forall h \in I/j, \forall j \in I, \forall t \quad (51)$$

$$R_j^{\text{CET}} + \sum_h R_{jh}^{\text{P2P}} \geq \sum_t (e^{\text{utility}} P_{j,t}^{\text{utility}} + e^{\text{GT}} P_{j,t}^{\text{GT}}) \quad \forall j \in I, \forall t \quad (52)$$

$$R_j^{\text{CET}} + \sum_h R_{jh}^{\text{P2P}} \geq 0 \quad \forall j \in I \quad (53)$$

$$P_{jh,t}^{\text{P2P}} + P_{hj,t}^{\text{P2P}} = 0 \quad \forall h \in I/j, \forall j \in I, \forall t \quad (54)$$

$$R_{jh}^{\text{P2P}} + R_{hj}^{\text{P2P}} = 0 \quad \forall h \in I/j, \forall j \in I, \forall t \quad (55)$$

where Eq. (51) establishes the foundational net load balance for an agent. Building upon this, Eq. (52) integrates environmental considerations by requiring that an agent's carbon quotas holdings are commensurate with or exceed their carbon emissions. To maintain the integrity of the carbon trading system, Eq. (53) ensures that carbon quota totals remain non-negative, thereby avoiding the scenario of deficit quotas.

4.2. Asymmetric Nash bargaining approach for market equilibrium

In the allocation of benefits among agents, the Asymmetric Nash Bargaining method is applied to explore the P2P energy trading pricing mechanism. Eq. (56) serves as the analytical tool to compute the optimal P2P energy transfer strategy, aimed at reducing the overall cost of the cooperative alliance. Furthermore, agent j 's electricity and carbon emission sales and purchases within an operational cycle can be

quantified and analyzed as follows:

$$\begin{cases} P_j^{\text{rec}} = \sum_t \sum_h \max(0, P_{jh,t}^{\text{p2p}}) \\ P_j^{\text{sup}} = \sum_t \sum_h \min(0, P_{jh,t}^{\text{p2p}}) \\ R_j = 1/(R^{\text{sum}} - R_j^{\text{sum}}) \end{cases} \quad \forall h \in I/j, \forall j \in I, \forall t \quad (56)$$

Here the contributions of agents in P2P energy trading are fully considered, recognizing the role of increased P2P electricity transactions in promoting real-time power balance. Carbon trading, as a policy-influenced mechanism, typically involves green energy producers who sell surplus quotas, thereby promoting green energy generation and consumption. Participation in P2P carbon quota transactions holds significant potential for energy conservation and emission reduction. This study proposes a carbon quota method based on marginal effect contribution, where an agent's impact is assessed by the change in the alliance's carbon quota. A smaller increase in the alliance's quota indicates a greater individual contribution by the agent, highlighting their positive influence on the broader energy network.

The study employs an exponential function with the natural constant e as its base to formulate a nonlinear mapping function for energy. This function serves the purpose of measuring the comprehensive contribution factor of agent j in terms of electricity and carbon emission trading, by their contribution to the collective sharing initiative.

$$\omega_j^P = 0.5 \left(\exp(P_j^{\text{sup}} / \sum_j P_j^{\text{sup}}) + \exp(P_j^{\text{rec}} / \sum_j P_j^{\text{rec}}) \right) \quad \forall j \in I \quad (57)$$

$$\omega_j^R = \exp(R_j / \sum_j R_j) \quad \forall j \in I \quad (58)$$

$$\omega_j = 0.7\omega_j^P + 0.3\omega_j^R \quad \forall j \in I \quad (59)$$

where agent j 's contributions to electricity and carbon emission trading are indicated by Eqs. (57) and (58), respectively. Considering the comprehensive contributions, electricity, as a demand-sensitive resource, is given priority in P2P transactions, while carbon trading, being policy-driven, is given a lower priority. Consequently, in the weighting process, the comprehensive contribution factor of electricity is weighted at 0.7, and that of carbon quota trading is weighted at 0.3.

After maximizing overall benefits, each agent engages in mutual negotiations to allocate the cooperative gains. The construction of an asymmetric benefit distribution model takes into account the comprehensive contribution factor of different agents.

$$\begin{cases} \max \prod_j (D_j^0 - D_j)^{\omega_j} \\ \text{s.t.} \quad D_j^0 \geq D_j \\ \lambda_{jh,t}^{\text{p2p}} - \lambda_{hj,t}^{\text{p2p}} = 0 \\ \mu_{jh}^{\text{p2p}} - \mu_{hj}^{\text{p2p}} = 0 \end{cases} \quad \forall h \in I/j, \forall j \in I, \forall t \quad (60)$$

where Eq. (60) introduces D_j^0 as the cost for agent j prior to P2P participation, acting as the negotiation breakdown threshold. Agent j 's post-transaction cost must be lower than D_j^0 to avoid negotiation failure.

A logarithmic linearization method [14] is employed to ensure the convexity of Eq. (60):

$$\begin{cases} \min -\omega_j \sum_j \ln(D_j^0 - D_j) \\ \text{s.t.} \quad D_j^0 \geq D_j \\ \lambda_{jh,t}^{\text{p2p}} - \lambda_{hj,t}^{\text{p2p}} = 0 \\ \mu_{jh}^{\text{p2p}} - \mu_{hj}^{\text{p2p}} = 0 \end{cases} \quad \forall h \in I/j, \forall j \in I, \forall t \quad (61)$$

The solution to the aforementioned issue is approached as a two-stage problem, consisting of the cooperative operation alliance subproblem P1 and the asymmetric benefit allocation subproblem P2. For

the cooperative operation alliance subproblem P1:

$$\begin{cases} \min \sum_j A_j \\ \text{s.t.} \quad (7)-(11), (13)-(40), (51)-(55) \end{cases} \quad \forall j \in I \quad (62)$$

where subproblem P1 aims to minimize the total cooperative alliance costs A_j for all agents, disregarding the P2P energy transaction costs B_j in the objective function. This exclusion is justified by the consideration that the total cost for all agents should be minimized. In P2P energy transactions, the prices for sellers and buyers are equal, which means that from the perspective of the cooperative alliance, the transaction costs for both buyers and sellers effectively cancel each other out.

By solving subproblem P1, we can obtain the optimal parameters for all variables except for the price. This lays the foundation for subproblem P2, which focuses on establishing the benefit allocation:

$$\begin{cases} \min -\omega_j \sum_j \ln(D_j^0 - A_j - C_j^{\text{p2p}} - E_j^{\text{p2p}}) \\ \text{s.t.} \quad D_j^0 \geq E_j^{\text{p2p}} + A_j - C_j^{\text{p2p}} \\ \lambda_{jh,t}^{\text{p2p}} - \lambda_{hj,t}^{\text{p2p}} = 0 \\ \mu_{jh}^{\text{p2p}} - \mu_{hj}^{\text{p2p}} = 0 \\ \lambda_t^{\text{p2p}} \leq \lambda_{jh,t}^{\text{p2p}} \leq \overline{\lambda}_t^{\text{p2p}} \\ \underline{\mu}^{\text{p2p}} \leq \mu_{jh}^{\text{p2p}} \leq \overline{\mu}^{\text{p2p}} \end{cases} \quad \forall h \in I/j, \forall j \in I, \forall t \quad (63)$$

To uphold market trading rules and avoid arbitrary energy pricing, while encouraging producers to prioritize transactions within cooperative alliances, it is ensured that transaction prices are in line with upper-level network prices, as per [58]. To preserve market stability and fairness, specific limits are set on the prices of electricity and carbon in each P2P transaction. With these constraints, the convex optimization problem is now ready for swift resolution by commercial solvers.

5. A fully decentralized PAC solution approach

The Nash bargaining framework for P2P energy trading discussed previously establishes a theoretical model for equitable and efficient market interactions. Building on this, the present section introduces a fully decentralized PAC approach, which reformulates the P2P trading optimization problem into a standard format compliant with atomic decomposition. This method ensures parallel computation and privacy by decentralizing the problem and applying a time-variant factor. By addressing constraint coupling and incorporating privacy measures, the PAC approach enhances the practical implementation of the Nash bargaining model in decentralized energy markets.

5.1. PAC solution modeling

For the convex optimization optimal problem established previously, this section will utilize the PAC algorithm to fully decentralize and solve the distribution system P2P energy trading optimization model presented in Eqs. (62) and (63) in parallel. To streamline the subsequent discourse and analysis, the problem is reformulated into the standard format of an optimization problem:

$$\begin{cases} \min f(y) \triangleq \sum_j f_j(y_j) \\ \text{s.t.} \quad Gy = b \end{cases} \quad \forall j \in I \quad (64)$$

The function $f(y)$ is assumed to be decomposable into a sum of multiple sub-functions $f_j(y_j)$; each $f_j(y_j)$ is referred to as the atomic problem of the s th atomic variable.

The complexity of power flow and P2P constraint coupling in the aforementioned problem is addressed by using an atomic decomposition method to decompose the problem in Eq. (64), into which is known

as the atomic problem:

$$D = (L, C, S, O, T) \quad (65)$$

where $L = \{L_j, \forall j \in K\}$ partition of N with $L_j \subseteq N$ being the components of y that each j th atom “owns”; $C = \{C_j, \forall j \in K\}$ partition of M with $C_j \subseteq M$ representing the rows of G that each j th atom “owns”; $S = \{S_j, \forall j \in K\}$ partition of F with $S_j \subseteq F$ representing the objective summands of f that each j th atom “owns”; $O = \{O_j, \forall j \in K\}$ each $O_j \subseteq Y$ representing the “copies” of variables of y additional to those of L_j that each j th atom needs to satisfy the scope of both G_{C_j} and $f_{S_j}(y) \triangleq \sum_k f_k(y)$; $T = \{T_j, \forall j \in K\}$ each $T_j = L_j \cup O_j \subseteq Y$ represents the total variables each j th atom “uses”.

By applying the atomic decomposition framework D , we can derive the standard atomic problem as follows:

$$\begin{cases} \min \sum_j f_j(a_j) \\ \text{s.t. } G_j a_j = b_j & \forall j \in I \\ B_{O_j} a = 0 \end{cases} \quad (66)$$

where G_j in the equation is the coefficient matrix for the j th atomic variable's equality constraints; For B , the expression is as follows:

$$B_i^m \triangleq \begin{cases} -1, & \text{if } i \text{ is "owned" and } m \text{ is a related "copy"} \\ 1, & \text{if } m \text{ is "owned" and } i \text{ is a related "copy"} \\ 0, & \text{otherwise} \end{cases} \quad (67)$$

where B_j and B^j indicate the in-degree and out-degree of an atom in a directed graph, respectively. A coordination constraint is added to enable full parallelization of the optimization, with each atom adhering to the second term of Eq. (64) to ensure equality of replicated variables among atoms.

5.2. P2P energy trading problem atomization and decoupling

In this section, the atomic framework introduced above is applied to the P2P energy trading problem that was established. For subproblem P1 (62), by introducing replicated variables for local atoms, the focus is on decoupling the branch flow constraints and the P2P energy trading constraints. For the branch flow model constraints:

$$\begin{cases} P_{j,t} = \sum_{i \in K} (P_{i,t} - l_{i,j,t} r_{ij}) - \sum_{k \in K} P_{j,k,t}^{[j]} \\ Q_{j,t} = \sum_{i \in K} (Q_{i,t} - l_{i,j,t} x_{ij}) - \sum_{k \in K} Q_{j,k,t}^{[j]} \\ V_{j,t} = V_{i,t}^{[j]} - 2(r_{ij} P_{i,t} + x_{ij} Q_{i,t}) + (r_{ij}^2 + x_{ij}^2) l_{i,j,t} \\ \left\| \begin{matrix} 2P_{i,t} & 2Q_{i,t} & l_{i,t} - V_{i,t}^{[j]} \end{matrix} \right\|_2 \leq l_{i,t} + V_{i,t} \end{cases} \quad \forall (i, j, k) \in B, \forall t \quad (68)$$

where the objective is to minimize the number of replicated variables to alleviate the communication burden. This decoupling is achieved by replicating the outflow active power $P_{j,k,t}^{[j]}$ and reactive power $Q_{j,k,t}^{[j]}$ of branches and by introducing the voltage of the upstream buses.

For the P2P energy trading constraints, it includes subproblem P1 and subproblem P2; for the subproblem P1:

$$\begin{cases} P_{j,h,t}^{p2p} + P_{h,j,t}^{p2p,[j]} = 0 \\ R_{j,h}^{p2p} + R_{h,j}^{p2p,[j]} = 0 \end{cases} \quad \forall h \in I/j, \forall j \in I, \forall t \quad (69)$$

where P2P electricity and carbon quotas trading replications with other agents facilitate decoupling. The first three terms in Eqs. (68) and (69) are succinctly encapsulated within the initial constraint of Eq. (66). The last term of Eq. (68) is maintained as the original constraint for the solution process.

For the subproblem P2:

$$\begin{cases} \lambda_{j,h,t}^{p2p} - \lambda_{h,j,t}^{p2p,[j]} = 0 \\ \mu_{j,h}^{p2p} - \mu_{h,j}^{p2p,[j]} = 0 \end{cases} \quad \forall h \in I/j, \forall j \in I, \forall t \quad (70)$$

Decoupling of subproblem P2, the focus is solely on decoupling the transaction prices, as the optimal power transmission and other variables have already been determined in subproblem P1.

As discussed in the previous section, the addition of coordination constraints is necessary. For the subproblem P1:

$$\begin{cases} P_{j,k,t}^{[j]} - P_{j,k,t} = 0 \\ Q_{j,k,t}^{[j]} - Q_{j,k,t} = 0 \\ V_{i,t}^{[j]} - V_{i,t} = 0 \\ P_{h,j,t}^{p2p,[j]} - P_{h,j,t}^{p2p} = 0 \\ R_{h,j}^{p2p,[j]} - R_{h,j}^{p2p} = 0 \end{cases} \quad \forall h \in I/j, \forall j \in I, \forall (i, k) \in B, \forall t \quad (71)$$

For the subproblem P2:

$$\begin{cases} \lambda_{h,j,t}^{p2p,[j]} - \lambda_{h,j,t}^{p2p} = 0 \\ \mu_{h,j}^{p2p,[j]} - \mu_{h,j}^{p2p} = 0 \end{cases} \quad \forall h \in I/j, \forall j \in I \forall t \quad (72)$$

where the coordination constraints are encapsulated in the second term of (66), signifying the completion of the decoupling for the subproblems P1 and P2.

5.3. Privacy-ensured PAC algorithm overall process

This section will present the Lagrangian function that forms the objective function for agent j as well as the update method for its dual variables, as shown in Algorithm 1.

Algorithm 1 Proximal Atomic Coordination (PAC) Algorithm

1: **Start**

2: **Initialization:**

Initialize all agents' variables $a_j[0]$, dual variables $\mu_j[0]$, $v_j[0]$, and proximal parameters ρ , γ_j
Set initial values for the Lagrange multipliers and iteration $\tau = 0$

3: **while** not converged **do**

4: **Local Variable Update:**

Each agent j solves its local subproblem to update $a_j[\tau + 1]$

5: **Privacy Protection:**

Using the formula (75), apply time-variant factor $\vartheta(\tau + 1)$ to update the local copies of the shared variables $\hat{a}_j[\tau + 1]$.

6: **Communication:**

Agents communicate the updated values to their neighbors

7: **Dual Variable Update:**

Update the dual variables $\mu_j[\tau + 1]$ and $v_j[\tau + 1]$ Using the formulae (76) and (78) and received $\hat{a}_j[\tau + 1]$.

8: **Privacy Protection:**

Using the formula (77) and (79), apply time-variant factors $\theta(\tau + 1)$ and $\epsilon(\tau + 1)$ to update the dual copies of the shared variables $\hat{\mu}_j[\tau + 1]$ and $\hat{v}_j[\tau + 1]$.

9: **Check Convergence:**

If the primal residuals $\|Ga[\tau] - b\|_2$ and the dual residuals $\|B_{O_j} a[\tau]\|_2$ are below a predefined threshold, proceed to the next step

Otherwise, increment τ and return to the step 4

10: **end while**

11: **End**

First, the proximal decomposition of the objective function is performed:

$$\begin{aligned} L(a, \mu, \nu_j) &= \sum_j \left[f_j(a_j) + \mu_j^T (G_j a_j - b_j) + \nu_j^T B_{O_j} a \right] \\ &= \sum_j \left[f_j(a_j) + \mu_j^T (G_j a_j - b_j) + \nu^T B^T a_j \right] \quad \forall j \in I \cup K \quad (73) \\ &\triangleq \sum_j L_j(a_j, \mu_j, \nu) \end{aligned}$$

Updates for local and dual variables are derived from the prox-linear Lagrangian function:

$$a_j[\tau + 1] = \operatorname{argmin} \left\{ L_j(a_j, \hat{\mu}_j[\tau], \hat{\nu}[\tau]) + \frac{1}{2\rho} \|a_j - a_j[\tau]\|_2^2 \right\} \quad \forall j \in I \cup K \quad (74)$$

$$\hat{a}_j[\tau + 1] = a_j[\tau + 1] + \vartheta(\tau + 1)(a_j[\tau + 1] - a_j[\tau]) \quad \forall j \in I \cup K \quad (75)$$

where communicating \hat{a}_j for all $j \in I \cup K$

$$\mu_j[\tau + 1] = \mu_j[\tau] + \rho\gamma_j(G_j \hat{a}_j[\tau + 1] - b_j) \quad \forall j \in I \cup K \quad (76)$$

$$\hat{\mu}_j[\tau + 1] = \mu_j[\tau + 1] + \theta(\tau + 1)\rho\gamma_j(G_j \hat{a}_j[\tau + 1] - b_j) \quad \forall j \in I \cup K \quad (77)$$

$$\nu_j[\tau + 1] = \nu_j[\tau] + \rho\gamma_j B_{O_j} \hat{a}_j[\tau + 1] \quad \forall j \in I \cup K \quad (78)$$

$$\hat{\nu}_j[\tau + 1] = \nu_j[\tau + 1] + \varepsilon(\tau + 1)\rho\gamma_j B_{O_j} \hat{a}_j[\tau + 1] \quad \forall j \in I \cup K \quad (79)$$

where communicating $\hat{\nu}_j$ for all $j \in I \cup K$

The algorithm iteratively updates the positive parameters ρ and γ_j and involves the protection of agent j 's variable a_j into \hat{a}_j using a time-variant factor $\vartheta(\tau + 1)$ in Eq. (75). The dual variables μ_j and ν_j are updated according to Eqs. (76) and (78). Subsequently, the protect dual variables $\hat{\mu}_j$ and $\hat{\nu}_j$ are updated using the time-variant factors $\theta(\tau + 1)$ and $\varepsilon(\tau + 1)$, based on Eqs. (77) and (79). Where $0 \leq \vartheta(\tau) \leq 1$, $0 \leq \theta(\tau) \leq 1$, $0 \leq \varepsilon(\tau) \leq 1$. The coupled agents communicate and protect variables to prepare for subsequent iterations. While the original PAC algorithm provides privacy only for the dual variables, the improved PAC algorithm ensures privacy for all communication variables [59].

6. Case study

The chosen case study is structured into four parts. Initially, the foundational data are presented and explained. Subsequently, a comparative analysis will be conducted between the PAC algorithm introduced herein and the ADMM algorithm. Following this, the decision-making process and the resulting outcomes of the model will be verified. Finally, an examination of how the credibility of renewable energy sources influences the P2P electricity and carbon trading mechanisms will be carried out.

6.1. Foundational data

All model establishment and solution search are performed on a computer with Windows 11 operating system, equipped with an AMD Ryzen Threadripper 3970X 32-Core Processor at 3.69 GHz and 64 GB of RAM. MATLAB R2018a and the YALMIP toolbox are utilized for all modeling tasks. In addressing the subproblem P1, denoted as an SOCP and presented in Eq. (62), the Gurobi 11.0.1 solver is selected due to its superior computational speed. Conversely, for the subproblem P2, which involves convex optimization with logarithmic functions and is detailed in Eq. (63). The Mosek 10.2.0 solver is deemed more appropriate owing to its specialized capabilities in this domain.

Fig. 3 illustrates the test case for this study, which includes a total of 10 agents (5 residential, 2 industrial, and 3 commercial). The positions and parameters of the loads are detailed in [49]. The distribution system allows a voltage magnitude range between 0.95 and 1.05 per

Table 2

Common parameter values for energy resource models with different agents.

Model	Parameter	Value
PV	r_r	1 kW/m ²
WT	v_c	3 m/s
	v_r	12 m/s
	v_o	25 m/s
MT	RD_j	-20% capacity
	RU_j	20% capacity
ESS	$\frac{P_j^{\text{ch}}}{P_j^{\text{dch}}}$	20% capacity
	$\eta^{\text{ch}}/\eta^{\text{dch}}$	95%
DR	$\frac{P_{j,t}^{\text{DR}}}{P_j^{\text{DR}}}$	-20% base load
	$\frac{P_j^{\text{DR}}}{P_j^{\text{DR}}}$	20% base load
Beta distribution	α	5
	β	1.5
Weibull distribution	c	15
	k	3

unit (p.u.), and the network usage charge for P2P energy trading is based on the actual values calculated in [60]. The carbon emissions from electricity purchased from the utility are derived from the 2021 electricity carbon dioxide emission factor data for China [61], with the base carbon quota price set at ¥90, reflecting recent carbon pricing trends. The typical daily load curve and electricity purchase and sale prices are illustrated in Fig. 4.

A multi-state probability model for wind speed and solar irradiance is generated based on [62,63]. Latin hypercube sampling is used to generate 5000 scenarios, which are reduced to 20 representative scenarios, as shown in Fig. 5. Considering the second-day real-time P2P energy trading, the parameters $\alpha = 0.5$ and $\alpha^* = 0.95$ are set, and α_+ is computed using Eq. (5) to be 0.4612. A detailed list of other parameters is provided in Tables 2 and 3.

6.2. Comparative analysis of different algorithms

This section presents a comparative analysis of four case scenarios defined by their optimization approach for P2P energy trading. This entails the following four methods:

Centralized Optimization: A conventional approach focusing on centralized decision-making for P2P energy trading.

ADMM: A fully decentralized application of the ADMM for P2P energy trading optimization, the formulae can be found in Appendix C.

PAC-Optimal: A fully decentralized PAC algorithm without privacy protection for P2P energy trading optimization.

PAC-Private: A fully decentralized PAC algorithm incorporating privacy protection for P2P energy trading optimization.

The method outlined in the literature [27] is utilized for the calculation of parameters ρ and γ for the PAC, as well as the parameter ρ for the ADMM. Convergence is defined as occurring when both the primal and dual residuals are less than 1×10^{-3} . The selection of initial values for the algorithms is achieved by introducing random perturbations around the optimal values for both the primal and dual variables. The distinction between PAC-Optimal and PAC-Private is characterized as follows:

- In PAC-Optimal, the values of all variables are determined by fixed optimal parameters at each iteration, providing a consistent approach to optimization.
- Conversely, PAC-Private introduces a time-variant factor of the primal and dual variables before each iteration's information exchange, ensuring privacy while maintaining the optimization process.

The results depicted in Fig. 6 present a comparative analysis of the coalition's total cost for subproblem P1 solved using the four

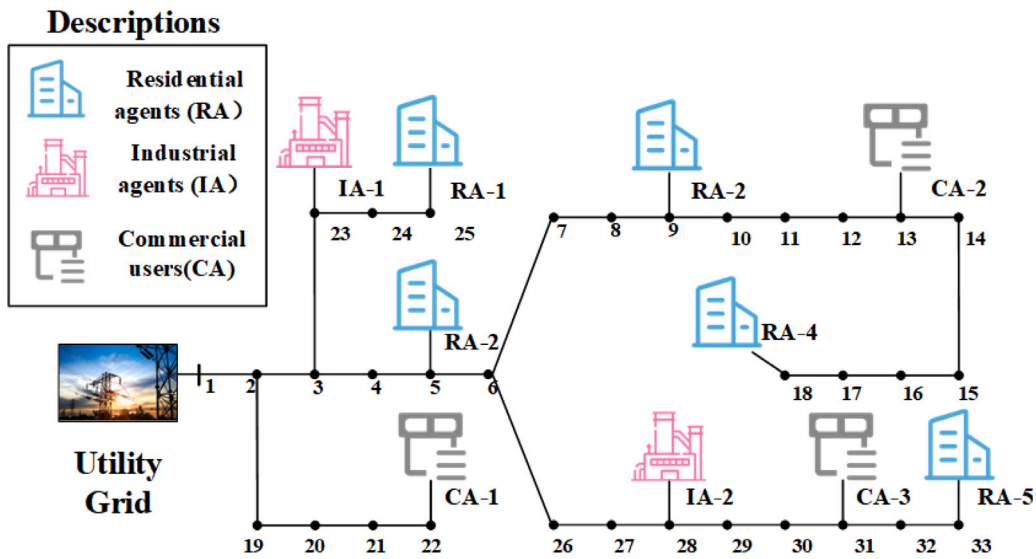


Fig. 3. IEEE 33 test feeders.

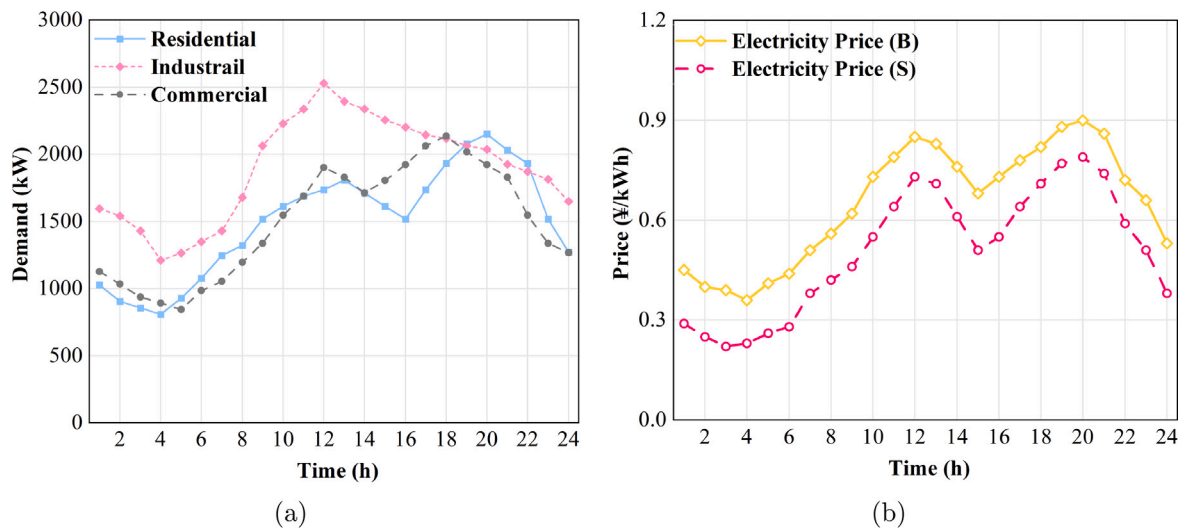


Fig. 4. Daily (a) Load curves for residential, industrial, and commercial sectors (b) Electricity purchase and sale prices from utility companies.

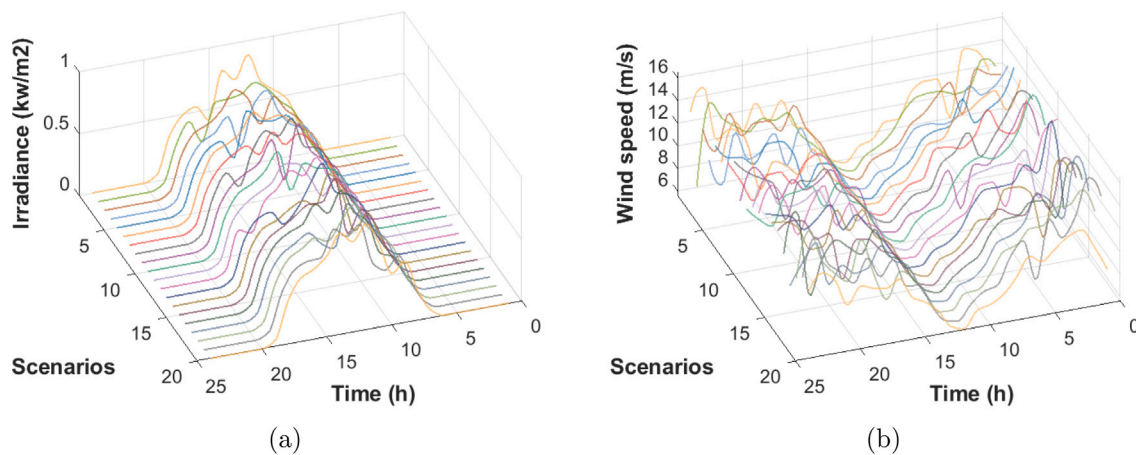


Fig. 5. Daily (a) Solar irradiance scenario diagram and (b) Wind speed scenario diagram.

Table 3
Summary of locations and installation capacities (kW) of generation units.

	Res. 1	Res. 2	Res. 3	Res. 4	Res. 5	Ind. 1	Ind. 2	Comm. 1	Comm. 2	Comm. 3
WT	×	×	×	×	×	1200	1400	×	×	×
PV	600	775	700	650	750	×	×	850	1000	1100
MT	×	×	×	×	×	800	800	500	500	500
ESS	250	400	320	300	350	700	800	×	×	×
DR	✓	✓	✓	✓	✓	✓	✓	✓	✓	✓

The terms “residential”, “industrial” and “commercial” are represented by the abbreviations “Res.”, “Ind.” and “Comm.”.

aforementioned algorithms. A total of 200 iterations are conducted to observe the outcomes. The black line represents the optimal total cost obtained using the Gurobi solver, amounting to ¥23,472.78. All three distributed algorithms converged to the optimal value around the 150th iteration. The PAC-Optimal algorithm demonstrated the fastest convergence rate, reaching the optimal value of ¥23,484.49 after 148 iterations. The ADMM algorithm achieved convergence at the 150th iteration with an optimal cost of ¥23,485.50. The PAC-Private algorithm completed convergence at the 155th iteration with a total cost of ¥23,485.26. Although real-time protection of variables enhances privacy, it somewhat impacts the optimal convergence rate of the PAC algorithm. In terms of iteration residuals, after 200 iterations, both the primal and dual residuals are below 1×10^{-3} , and the algorithms exhibited less oscillatory behavior compared to ADMM.

The average computational time for both PAC-Optimal and PAC-Private is 0.82 s, with maximum times recorded at 1.11 s. In contrast, ADMM exhibits an average computational time of 0.97 s, peaking at a maximum of 1.35 s. Disregarding communication delay, the total solution time achieved through parallel computation is as follows: PAC-Optimal completes in 121.36 s, while ADMM takes 145.51 s. PAC-Private, despite the additional step of real-time protected, concludes in 127.11 s, compared to ADMM, the PAC-Private total computation time has been reduced by 12.65%. In brief, in terms of total computational time, the PAC-Optimal algorithm outperforms both PAC-Private and ADMM, primarily due to its lowest iteration count and the shortest computational time per attempt. Despite having a slightly higher iteration count compared to ADMM, PAC-Private achieves a better total time due to its lower average computational time per attempt, which compensates for the additional iterations. PAC-Private, while offering enhanced privacy through time-variant factors, incurs a slight increase in total computational time compared to PAC-Optimal, indicating a trade-off between privacy protection and computational efficiency.

Based on the aforementioned comparison, the PAC-Private algorithm is employed to solve the asymmetric Nash bargaining subproblem P2, as it effectively protects the trading price information in the P2P energy trading, with a total of 300 iterations conducted. A centralized solution, serving as a benchmark, is obtained by invoking the Mosek solver. From the iteration information in Fig. 7, all agents achieve convergence by the 229th iteration, the detailed results of each agent can be found in Appendix D, with the following total costs for each type of agent: residential agents at ¥9882.13, industrial agents at ¥900.38, and commercial agents at ¥12,690.18. The average computational time per iteration is 0.62 s, accumulating to a total duration of 141.98 s.

In summary, the PAC-Private algorithm’s strength lies in its implementation of time-variant protection for all communicated primal and dual variables, thereby enhancing data security and privacy protection. This protection method makes it highly challenging to revert to the original values [27], ensuring the confidentiality of agents’ data in a distributed environment. Specifically, \hat{v}_j serves as a coordination factor between different agents, responsible for ensuring the overall cost optimization within a cooperative alliance. During the solution process of the subproblems, \hat{v}_j plays a different but equally crucial role in both subproblem P1 and subproblem P2. For subproblem P1, \hat{v}_j contains key information that ensures the optimal transfer of energy across the cooperative alliance, allowing the system to achieve the optimal distribution of energy among different agents and prevent imbalances

in power transfer, minimize the total operating cost of the cooperative alliance. For subproblem P2, \hat{v}_j carries optimal pricing information between agents, leading to fairer and more reasonable transaction prices within the alliance, realize the distribution of benefits within the cooperative alliance. However, for other methods described beside the PAC-Private algorithm, \hat{v}_j is not effectively protected. If its value is tampered with, there is a risk of imbalance in the energy distribution of the cooperative alliance and unfairness in the transaction prices of the agents, thereby harming the interests of the alliance as a whole and each agent. Overall, the PAC-Private algorithm adopted in this paper has achieved satisfactory results in solving both subproblem P1 and subproblem P2.

6.3. Analysis of P2P energy trading results

The analysis of the P2P electricity, as depicted in Fig. 8, reveals distinct patterns throughout the day: **Low-Demand Period (0:00–8:00)**: During the early morning hours, the P2P electricity trading volume is observed to be low. This is primarily due to the reduced demand for electricity during this time. Additionally, the absence of solar irradiance and higher wind speeds after midnight mean that PV cannot generate electricity, leaving industrial agents as the sole producers who prefer to engage in P2P energy trading with commercial agents rather than residential agents. **Morning to Afternoon Period (9:00–16:00)**: As daylight and wind conditions change, the electricity generation from PV increases. Residential and commercial agents transform into energy producers, while industrial agents become consumers. **Evening Peak Demand (17:00–24:00)**: With the ending of PV power generation in the evening and a peak in electricity demand between 19:00 and 21:00, the cost of purchasing electricity from utility companies is high due to time-of-use pricing policies. Consequently, the P2P electricity trading volume reaches its peak during this period. Industrial agents revert to being electricity producers, while residential and commercial agents turn into consumers.

Evaluating the decision-making mechanisms of various agents across different time segments reveals different energy management strategies. As illustrated in Fig. 9, during the early morning hours, residential agents primarily satisfy their electricity needs by purchasing from utility companies rather than relying on P2P energy trading. This is attributed to the fact that renewable energy generation at night comes mainly from wind power, and all agents favor energy consumption during lower-priced nighttime slots to maximize their benefits. Commercial agents, to meet their load demands, purchase electricity not only through P2P trading with industrial agents but also from utility companies.

Both residential and industrial agents opt to charge their ESS during the early morning period. As the day progresses, with the increase in PV generation, the electricity supply for residential and commercial agents primarily shifts to solar power. In the peak mid-day period (12:00–14:00), when solar generation reaches its peak, these agents sell their surplus electricity to industrial agents. Industrial agents, in addition to wind power and P2P energy trading, also increase their power generation from MT to meet their load demands during the period.

As evening approaches and PV generation decreases to zero, the peak demand period from 19:00 to 21:00 sees MTs of both industrial

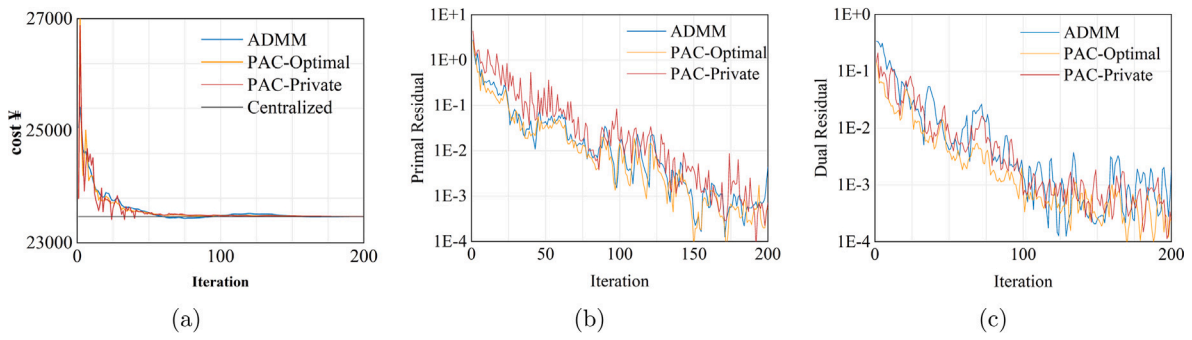


Fig. 6. Convergence chart of algorithms for (a) Cost, (b) Dual residual, and (c) Primal residual.

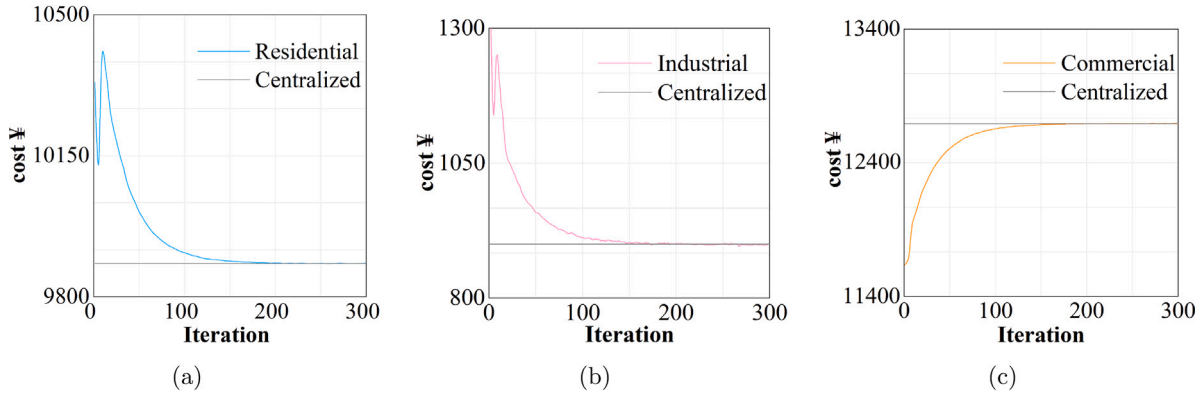


Fig. 7. Convergence chart of cost allocation based on the PAC-Private algorithm for (a) Residential agents, (b) Industrial agents, and (c) Commercial agents.

and commercial agents operating at maximum capacity. This strategy is employed because the cost of generating electricity using MTs during this period is lower than the cost of purchasing from utility companies. ESSs also discharge during these hours. By the time it reaches 22:00 to 24:00, with the reduction in electricity demand, the volume of P2P electricity trading correspondingly declines.

The impact of P2P electricity trading on the distribution system has been assessed, and the results depicted in Fig. 10(a) demonstrate that the proposed trading mechanism effectively ensures the secure and stable operation of the system. The lowest voltage magnitudes are notably concentrated at buses 13 to 18, as shown in Fig. 10(a). This phenomenon can be attributed to the period when PV generation is inactive, leading to commercial agent 2 and residential agents 3 and 4 operating solely as energy consumers. The absence of local renewable energy compensation, coupled with the extended lengths of the associated branches, results in significant voltage drops and consequently lower voltage magnitudes. Upon examination of the line loading rates in Fig. 10(b), it is observed that during peak electricity demand periods, the line loading rates of the distribution system increase accordingly, due to the marked increase in power transmission volumes. Particularly in the early morning, when residential and commercial agents primarily meet their demand by purchasing electricity from the utility company, the loading rates of lines close to the first node are higher. Similarly, during the evening peak demand period from 19:00 to 21:00, the surge in electricity demand makes P2P electricity trading an essential means to satisfy load requirements, resulting in higher overall line loading rates in the distribution system. However, at all times, the method used in this article effectively limits the voltage and line loading rates within safe ranges.

The subsequent evaluation of the cost allocation under the trading framework proposed in this paper is presented in Fig. 11. Compared to the scenario without P2P energy trading, where the total cost is ¥26,165.21, the introduction of P2P energy cooperation has resulted

in a total cost of ¥23,472.78, reflecting a 10.29% reduction. Meanwhile, the total carbon quota is 28.45t without P2P energy trading. Conversely, the total carbon quota is 25.43t with P2P energy trading, reflecting an 11.86% reduction. For the cost allocation among various agents, a comprehensive contribution factor calculation formula as shown in Eq. (59) has been applied to determine each agent's contribution. The resulting comprehensive contribution factors for residential agents 1–5 are 1.12, 1.10, 1.11, 1.11, and 1.10, respectively. For industrial agents 1 and 2, the factors are 1.20 and 1.21, respectively; and for commercial agents 1–3, they are 1.04, 1.05, and 1.06, respectively. Based on these comprehensive contribution factors, the final total costs for each agent have been calculated. The proportion of total costs for residential and industrial agents has decreased, indicating a higher contribution to the prosumer alliance. Conversely, the lower proportion of costs for commercial agents suggests a comparatively lower contribution relative to residential and industrial agents. The greatest reduction in the proportion of total cost after negotiation is experienced by industrial agent 1, with a decrease of 1.03%. Meanwhile, the highest increase in cost proportion is observed for commercial agent 3, with an increase of 0.96%.

To visually present the bargaining ability of each agent and the flow of transactions, the P2P electricity trading at noon 12:00 and evening 19:00, as well as the full-day P2P carbon emission trading, are analyzed, with results shown in Fig. 12. At noon, with enough PV power generation, at the price when industrial agents, as consumers within the alliance, purchase electricity from residential agents is generally higher than that from commercial agents. As evening approaches, with sufficient wind power generation, the selling price of industrial agents to commercial agents is generally higher than that to residential agents.

In the case of P2P carbon emission trading, the price difference between industrial and commercial agents is more pronounced. This is due to the tiered carbon pricing involved in carbon emission transactions. As depicted in Fig. 12(c), commercial agents have a larger load

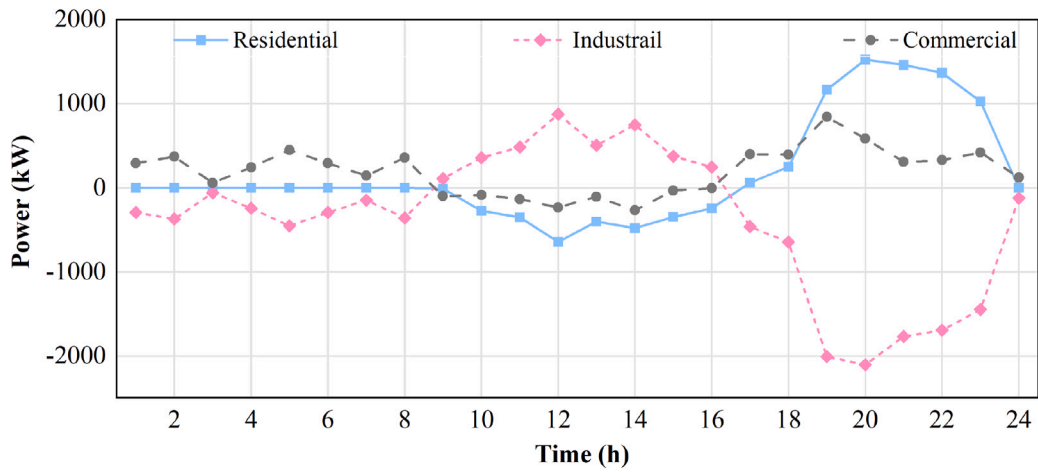
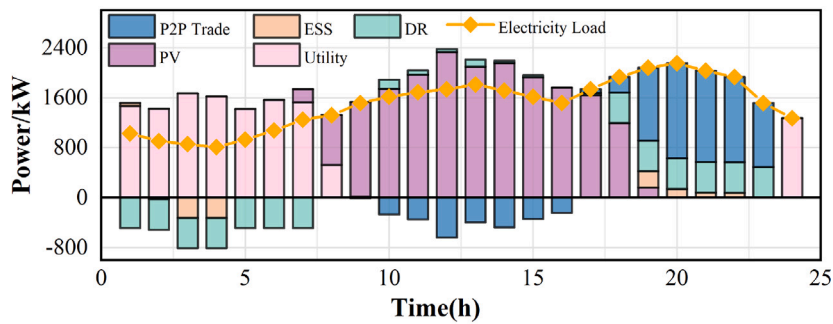
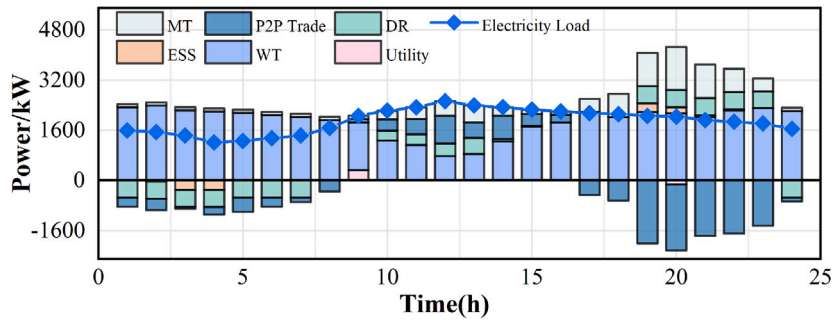


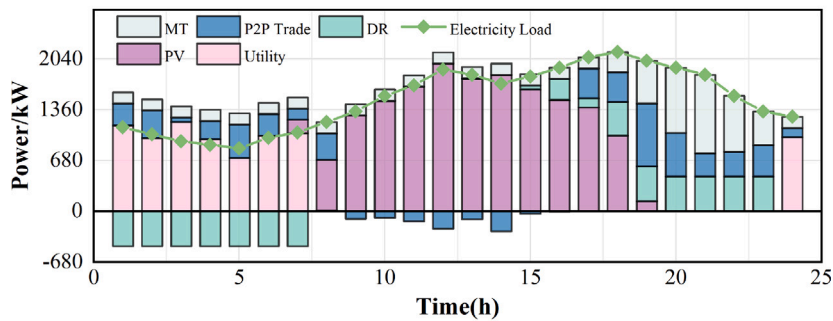
Fig. 8. Overall power results of the P2P electricity trading.



(a)



(b)



(c)

Fig. 9. Detailed power results of P2P electricity trading for agents: (a) Residential agents, (b) Industrial agents, (c) Commercial agents.

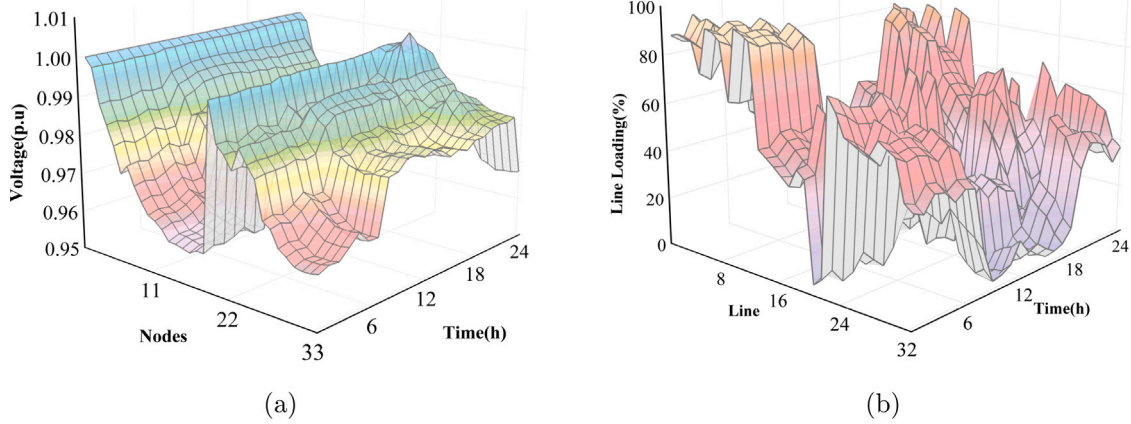


Fig. 10. Test the voltage amplitude of all buses in the testing system (a), Line loading of all branches (b).

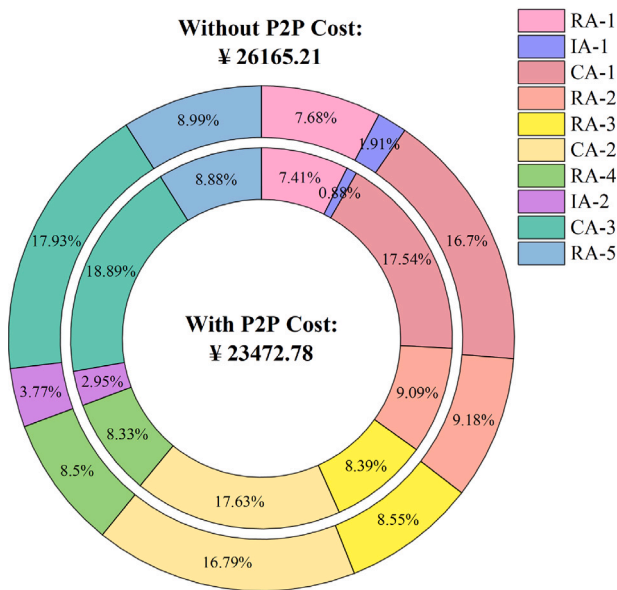


Fig. 11. Cost allocation among agents with and without P2P energy trading.

and insufficient photovoltaic capacity, necessitating the purchase of a significant amount of carbon quotas to meet their energy needs through electricity from the utility company and MT power generation. Consequently, under the tiered carbon trading mechanism, industrial agents are more inclined to sell electricity to commercial agents, as selling green power to them indeed reduces the total cost of the prosumer alliance. Additionally, residential agents purchase extra carbon quotas beyond their own needs for resale. However, both buyers and sellers benefit from P2P carbon emission trading.

The results depicted in Fig. 13 provide an in-depth analysis of the P2P electricity trading prices at various times, combining the lower and upper bounds. It can be observed that during the 9:00–17:00 period, P2P electricity trading prices tend to lean toward the lower limit, while for the periods of 0:00–8:00 and 18:00–24:00, the P2P electricity trading prices lean more toward the upper limit. The outcomes indicate that regardless of whether the industrial agents act as energy producers or consumers, they can secure greater profits. This advantage stems from the industrial agents’ significant comprehensive contribution factor, which arises from their extensive purchasing and selling of electricity and CET. This, in turn, gives industrial agents stronger bargaining ability in the P2P energy market.

Table 4
Solution time under 4 different model in PAC algorithm.

Model	Solution time for different sample sizes/s				
	500	1000	2000	5000	10 000
SP	252.65	320.85	437.10	652.55	1266.82
DRO-W	146.35	158.96	171.72	188.34	254.39
DRCC-KL	127.48	127.36	126.95	127.11	127.08
RO	105.77	107.37	113.34	124.22	133.53

6.4. Comparative analysis of different confidence levels

To investigate the impact of different uncertainty optimization models on the results, this study constructs the following four models:

SP: This model optimizes based on a scenario set generated through extensive sampling, and its formulation is presented in (A.11).

RO: This model ensures feasibility across all scenarios and is formulated as shown in (A.3).

DRO-W: Following the approach in [39,64], this model uses the Wasserstein-metric-based DRO framework. Affine decision rules are adopted to adjust the modeling process, where sampled scenarios are treated as error vectors and incorporated into a data-driven support set through the Dirac distribution. The confidence level is set to 0.9.

DRCC-KL: This model is proposed in this study with parameters set at a confidence level of $\alpha = 0.9$ and $\alpha^* = 0.95$.

Fig. 14 presents the economic results for the four models described above. For the SP model, the coalition’s total cost is ¥35,125.09, with a total carbon quota of 36.80 tons. Under the RO model, the coalition’s total cost increases to ¥39,579.12, with a total carbon quota of 40.54 tons. The DRO-W model results in a total cost of ¥36,651.46 and a carbon quota of 48.43 tons, whereas the DRCC-KL model achieves a total cost of ¥36,078.95 and a carbon quota of 37.72 tons. The cost for all agents under the DRCC-KL model is lower than that under the RO and DRO-W models but higher than under the SP model. The SP model, which only considers the reference probability distribution of renewable energy, lacks robustness as it inadequately addresses extreme scenarios, resulting in overly optimistic optimization costs. The RO model, on the other hand, focuses solely on the worst-case scenarios, disregarding probability distribution information, leading to overly conservative outcomes. The DRO-W model, due to the adoption of affine principles and dual transformations, cannot guarantee the accuracy of transformed results [44], thus yielding more conservative results compared to the DRCC-KL model.

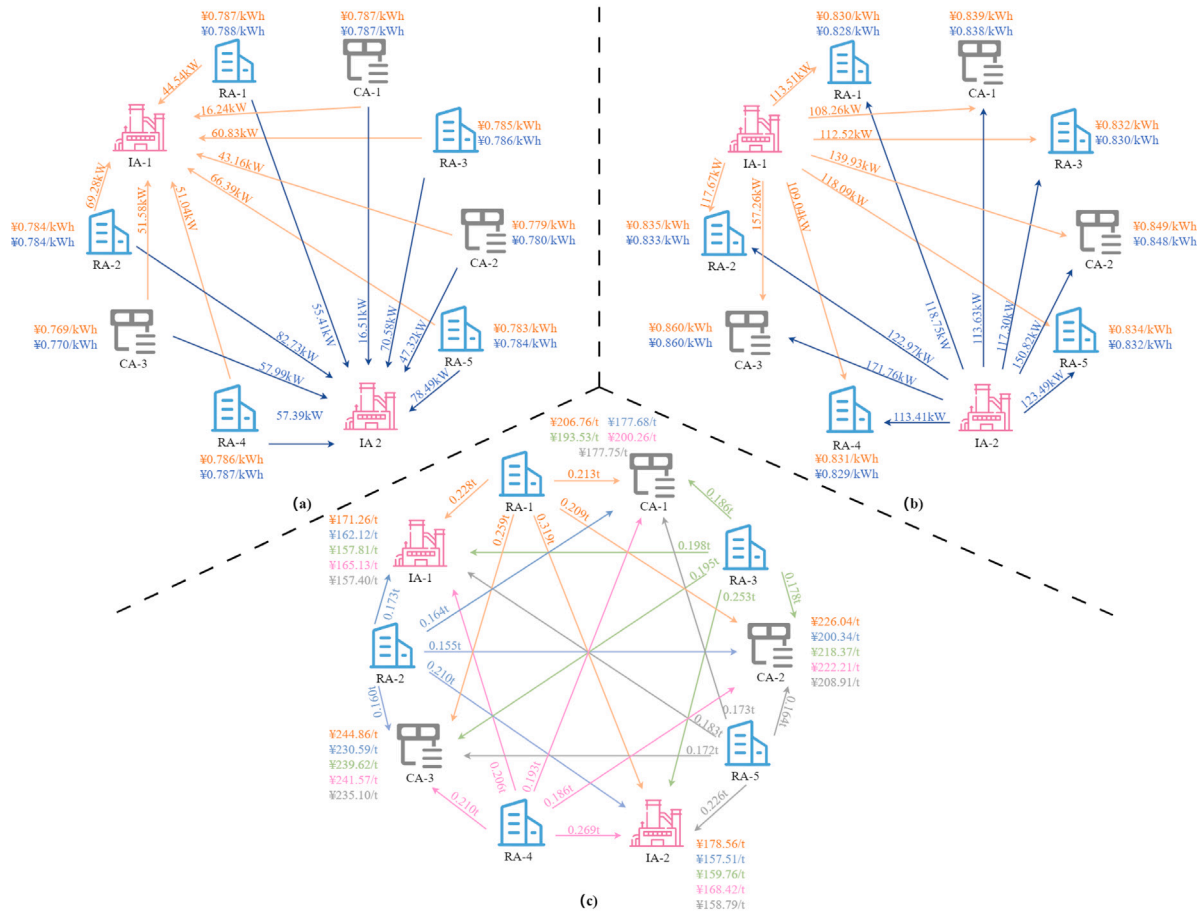


Fig. 12. P2P electricity trading flow and prices at (a) Noon 12:00, (b) Evening 19:00 and (c) Full-Day P2P carbon emission trading flow and prices.

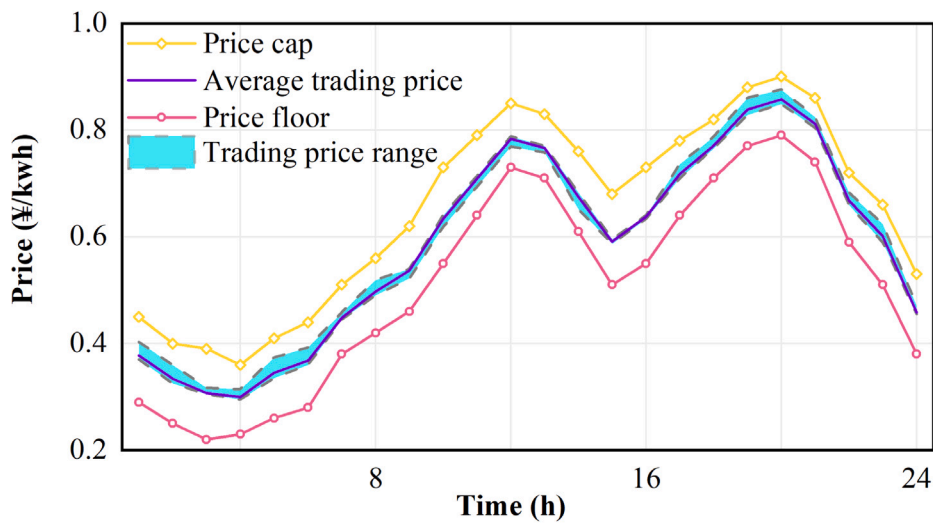


Fig. 13. Price ranges for P2P electricity trading at various times.

Table 4 compares the computation times for the four models after convergence using the PAC algorithm. The SP model requires processing all historical data samples, causing its computation time to increase with the number of samples, when the number of samples is 10000, it takes 1266.82 s. In contrast, the RO model, which only identifies the worst-case scenario, has the fastest computation speed among the

four models. The DRO-W model, which requires identifying additional boundary values within scenarios, is slightly slower than the RO model. In the DRCC-KL model, leveraging the proposed multi-state generation model to reduce the number of scenarios, the calculation time is always around 127 s, it does not change with the increase of sample size due to its clustering-based confidence result calculations.

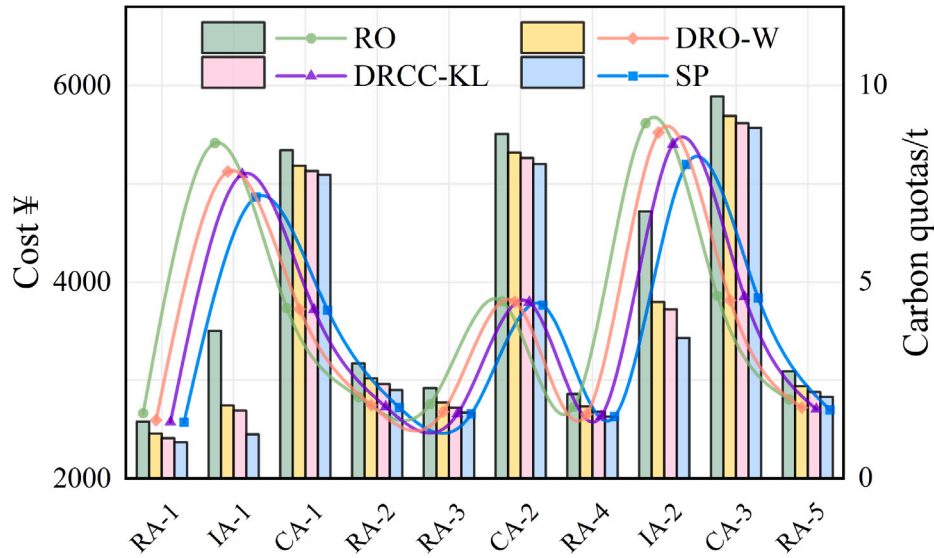


Fig. 14. Comparison costs and carbon quotas under 4 different model.

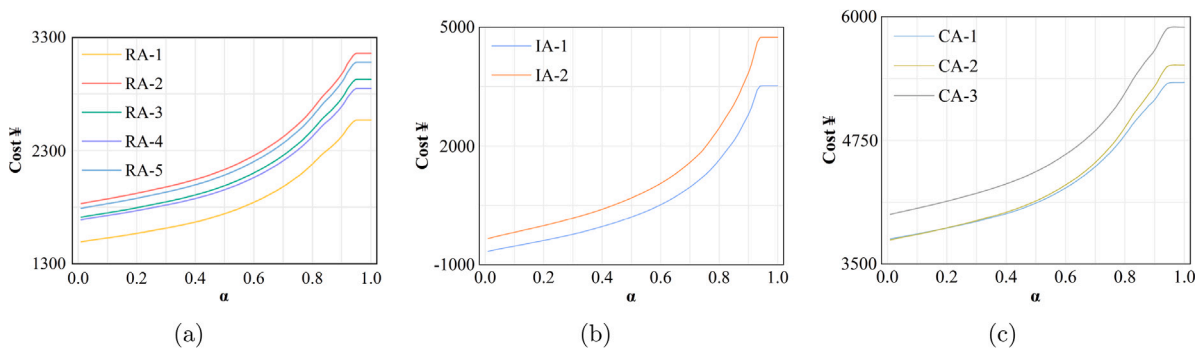


Fig. 15. Variation of agent costs with reliability levels, (a) Residential agent, (b) Industrial agent and (c) Commercial agent.

Table 5 presents an analysis of the impact of varying the confidence level of the probability density function, denoted as α^* , and the number of scenarios M , on the total cost of the prosumer alliance under a constant distributionally robust reliability level of $\alpha = 0.5$. The analysis reveals that as the d_{KL} value increases, the optimized cost also increases, indicating a more conservative optimization outcome with enhanced robustness. By maintaining a fixed confidence level of α^* and increasing the number of scenarios M , the optimization cost gradually decreases. This suggests that incorporating more historical data allows the reference distribution to more closely approximate the actual distribution, thereby mitigating the risk of extreme low-probability events and reducing the total cost for the prosumer alliance. Collectively, these findings indicate that increasing the number of generated scenarios has a more pronounced effect on optimization costs compared to altering the value of α^* , and represents a more effective method for improving economic efficiency.

The subsequent evaluation examines the impact of the distributionally robust reliability level α on the costs of various agents under constant confidence levels of the probability density function α^* and a fixed number of scenarios M , as depicted in Fig. 15. By increasing α from 0 to 1, it is observed that the cost for each agent increases significantly. At $\alpha = 0$, the chance constraint of the DRCC model has a failure probability of 1, indicating no consideration of worst-case

scenarios of renewable energy generation. Conversely, at $\alpha = 1$, the failure probability of the chance constraint is 0, accounting for all worst-case scenarios of renewable energy. Moreover, at $\alpha = 0$, the costs for commercial agents 2 and 3, and residential agents 3 and 4 are similar. However, as α increases, the cost disparity between these two sets of agents widens. This is attributed to the larger renewable energy installation capacities of residential agent 3 and commercial agent 2, compared to the smaller capacities of residential agent 4 and commercial agent 3. The selection of the α value has a more pronounced impact on agents with larger installation capacities. Therefore, when formulating energy trading and management strategies, the wise choice of α is crucial for agents with significant installation capacities to balance cost and risk management effectively.

The final assessment investigates the impact of the distributionally robust reliability level α on P2P energy trading while keeping the confidence level of the probability density function α^* and the number of scenarios M constant, as illustrated in Fig. 16. It is observed that as the value of α increases, the volume of electricity transactions increases at various times. However, at certain moments, the electricity trading volume exhibits a decrease followed by an increase with the rise in α . This phenomenon occurs when the generation of renewable energy is nearly equal, leading to an ambiguity in the roles of sellers and buyers at that moment, thus causing a temporary reduction in P2P electricity

Table 5
Impact of uncertainty under different parameters.

M	α^*	$\alpha^* = 0.90$		$\alpha^* = 0.95$		$\alpha^* = 0.99$	
		d_{KL}	Cost ¥	d_{KL}	Cost ¥	d_{KL}	Cost ¥
	500	0.0272	24 753.55	0.0301	24 866.98	0.0362	25 089.06
	1000	0.0136	24 153.61	0.0151	24 226.79	0.0181	24 370.10
	2000	0.0068	23 767.27	0.0075	23 815.07	0.0090	23 907.11
	5000	0.0027	23 443.71	0.0030	23 472.78	0.0036	23 527.25
	10 000	0.0014	23 287.32	0.0015	23 306.93	0.0018	23 344.76

trading. In terms of P2P carbon emission trading, the quota of CET decreases progressively with the increase in α . This trend indicates that enhancing the utilization of renewable energy can effectively reduce agents' carbon emissions. A compensatory relationship is observed between CET and electricity trading, where a decrease in CET quota corresponds to an increase in electricity trading volume.

For decision-makers in the energy sector, the adoption of the decentralized PAC approach for P2P energy trading offers significant practical advantages. Implementing this framework can enhance market efficiency and equity by leveraging parallel computation, which ensures faster transaction processing compared to traditional methods like ADMM. Additionally, the PAC-Private variant provides robust privacy protections for all communication variables, addressing critical concerns about data security and fostering greater trust among participants. This is particularly important in distributed energy markets where the confidentiality of agents' data is paramount. Furthermore, decision-makers should also note the positive environmental impact, as the framework supports higher utilization of renewable energy sources, leading to reduced carbon emissions and aligning with sustainability goals. By integrating these insights, policymakers and energy managers can design more resilient, efficient, and secure P2P energy trading systems that not only lower operational costs but also contribute to environmental sustainability. Emphasizing the balance between computational efficiency and privacy protection will be key to successfully deploying decentralized energy markets and achieving broader energy transition objectives.

7. Conclusion and future work

This research investigate the behavior decision-making, profit distribution, and fully decentralized implementation with privacy protection of various types of agents participating in P2P electricity and carbon markets under the premise of considering the uncertainty of renewable energy. Here the following conclusions are drawn:

The extension of market dynamics through cooperative alliance-based modeling combined with the asymmetric Nash bargaining approach uncovers the fair distribution of transaction costs of P2P electricity and carbon allowances. Using these models resulted in a reduction in carbon quota by 3.02 tons and a cost decrease of 2692.43, demonstrating their efficacy in improving both economic and environmental performance. These models intricately capture the cost structures of energy production and trading.

Building upon this foundation, the fully decentralized PAC algorithm emerges as a scalable solution for optimizing P2P energy trades without the need for a central supervisor, thereby safeguarding privacy. In comparison to the widely adopted ADMM algorithm, the PAC algorithm reduces computational time by 87.35%, showcasing significant improvements in convergence speed and efficiency. This decentralized approach ensures practical applicability in real-world scenarios where data privacy and solving efficiency are critical for P2P energy trading.

Furthermore, the integration of uncertainty in distributed generation is essential for enhancing the absorption of renewable

energy resources and mitigating carbon emissions within P2P energy trading. Models developed for assessing the uncertainty associated with renewable energy resources emphasize the importance of robust probabilistic frameworks to enhance the reliability of energy trading markets. The approach harnesses KL divergence to effectively model uncertainty sets, providing a sound basis for decision-making subject to significant uncertainty factors.

Finally, future work on P2P energy trading should focus on improving the accuracy of renewable energy uncertainty characterization. Integrating advanced techniques such as integrated risk measurement-based stochastic optimization [65] and info-gap decision theory [66] into fully decentralized PAC algorithms represents a crucial avenue for further exploration.

CRedit authorship contribution statement

Chengwei Lou: Writing – original draft, Supervision, Conceptualization. **Zekai Jin:** Writing – original draft, Software. **Yue Zhou:** Writing – review & editing. **Wei Tang:** Writing – review & editing. **Lu Zhang:** Project administration. **Jin Yang:** Writing – review & editing, Funding acquisition.

Declaration of competing interest

The authors declare that they have no known competing financial interests or personal relationships that could have appeared to influence the work reported in this paper.

Acknowledgment

The work is supported by the Engineering and Physical Sciences Research Council (EPSRC, United Kingdom) in project ‘‘Street2Grid - an electricity blockchain platform for P2P energy trading’’ (Reference: EP/S001778/2).

Appendix A. Convert DRO model to chance-constrained model

The DRO model provides a balanced approach to uncertainty and conservatism in contrast to the SP and RO models, with a more adaptive handling of uncertainty. The DRO model for renewable energy output can be formulated as follows:

$$\inf_{P \in \sigma} \Pr \{h(\xi) \leq 0\} \geq 1 - \alpha \quad (\text{A.1})$$

The SP model considers the reference probability density of renewable energy, with its formulation presented below:

$$\Pr_0 \{h(\xi) \leq 0\} \geq 1 - \alpha \quad (\text{A.2})$$

The RO model optimizes for the worst-case scenario of renewable energy sources, with its formulation presented below:

$$\max_{\xi} h(\xi) \leq 0 \quad (\text{A.3})$$

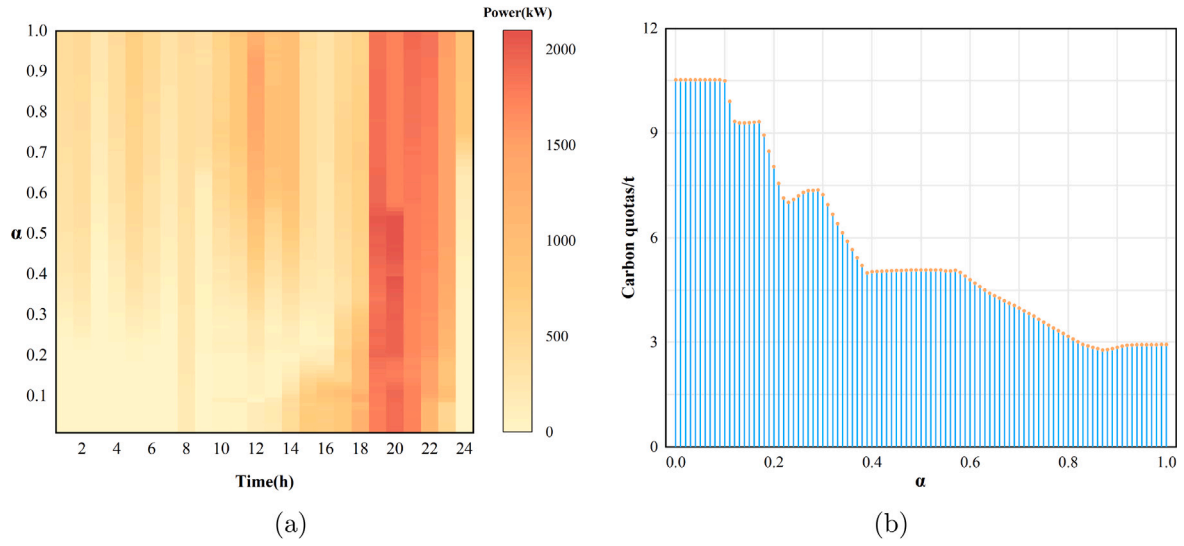


Fig. 16. Under the variation of reliability levels: (a) P2P electricity transaction volume, (b) CET quotas.

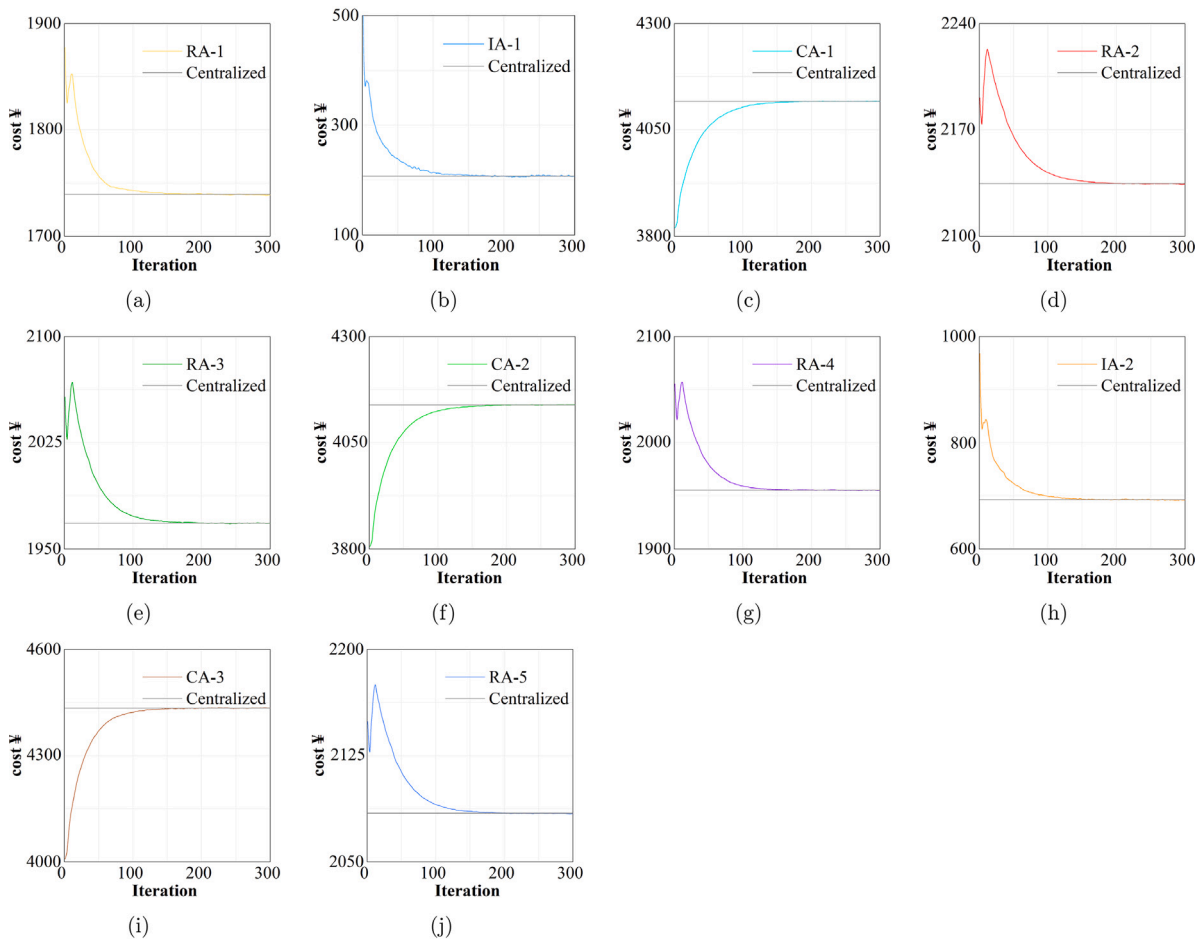


Fig. D.17. PAC-Private convergence of sub-problem P2 (a) RA-1, (b) IA-1, (c) CA-1, (d) RA-2, (e) RA-3, (f) CA-2, (g) RA-4, (h) IA-2, (i) CA-3, (j) RA-5.

where the ξ is used to denote uncertainty variables across the three models, This includes wind speed and solar irradiance. The DRO model, which fuses features of SP and RO, is designed to address the worst-case scenarios within the probability distribution.

The DRO problem is challenging to handle probabilistic distribution constraints. However, when the problem is characterized using KL divergence, as referenced in [52], the DRO model is transformed into a conventional chance-constrained model.

$$\Pr_0\{h(\xi) \leq 0\} \geq 1 - \alpha_+ \quad (\text{A.4})$$

Due to the non-convex chance constrained in Eq. (A.4) remaining challenging to solve, this paper uses an approach to find a convex conservative approximation for the optimization problem. The following equivalent transformation is applied to Eq. (A.4):

$$\Pr_0\{h(\xi) > 0\} = E_{p_0}(I_+(h(\xi))) \leq \alpha_+ \quad (\text{A.5})$$

$$I_+(x) = \begin{cases} 1 & x > 0 \\ 0 & x \leq 0 \end{cases} \quad (\text{A.6})$$

The expression is approximated by introducing a convex function $\psi(x)$ to replace $I_+(x)$, thereby scaling the expression.

$$\psi(x) = \max\{0, x/\beta + 1\} \quad (\text{A.7})$$

$$E_{p_0}(I_+(h(\xi))) \leq E_{p_0}(\psi(h(\xi))) \leq \alpha_+ \quad (\text{A.8})$$

In the subsequent steps, the SAA method is utilized to solve the expected value term of Eq. (A.8). Assuming the n th sample ξ_n has a probability of π_n , the expected value of Eq. (A.8) is determined as follows:

$$\sum_n \pi_n \max\{0, h(\xi_n)/\beta + 1\} \leq \alpha_+ \quad \forall n \quad (\text{A.9})$$

where the introduction of the auxiliary variable ϕ_n serves to completely transform the derived DRO model into the following linear DRCC model:

$$\begin{aligned} h(\xi_n) + \beta &\leq \phi_n, & \phi_n &\geq 0 \\ \sum_n \pi_n \phi_n &\leq \beta \alpha_+, & \beta &> 0 \end{aligned} \quad \forall n \quad (\text{A.10})$$

The SP model can be transformed into the following linear model:

$$\begin{aligned} h(\xi_n) + \beta &\leq \phi_n, & \phi_n &\geq 0 \\ \sum_n \pi_n \phi_n &\leq \beta \alpha, & \beta &> 0 \end{aligned} \quad \forall n \quad (\text{A.11})$$

Appendix B. Algorithm for constructing multi-state probability models using latin hypercube sampling

See Algorithm 2.

Appendix C. ADMM algorithm based on atomization framework for distributed optimization

In Refs. [27,67], a ADMM algorithm based on atomization framework is formed, and its formula is as follows

$$a_j[\tau + 1] = \operatorname{argmin} \left\{ \begin{aligned} &L_j(a_j, \mu_j[\tau], \nu[\tau]) + \frac{\rho}{2} \|G_j a_j - b_j\|_2^2 \\ &+ \frac{\rho}{2} \|B^{Tj}(a_j - a_j[\tau] + w[\tau])\|_2^2 \end{aligned} \right\} \quad \forall j \in I \cup K \quad (\text{C.1})$$

where communicate a_j for all $j \in I \cup K$

$$\mu_j[\tau + 1] = \mu_j[\tau] + \rho(G_j a_j[\tau + 1] - b_j) \quad \forall j \in I \cup K \quad (\text{C.2})$$

Algorithm 2 Multi-State Probability Model

- 1: **Start**
- 2: **Initialization:**
Set the calculation precision, initial number of cluster centers N_c , max probability models N_{\max} , probability models $N_p = 1$
- 3: **Generate Sample**
Generate samples based on the Latin Hypercube Sampling method.
- 4: **Model Setup:**
- 5: **while** The new curve is not the same as the cluster center **do**
Determine the cluster centers for the wind speed and irradiance curve states according to $l_1' = l_{\max}, l_2' = l_{\min}, l_a' = l_e, a = 3, \dots, N_c, e = 1, \dots, N_c - 2$
- 6: Calculate the distance from each sample to the cluster centers using $d_{b,a} = \sqrt{\sum_t (l_{b,t} - l_{a,t}')^2}$
- 7: Assign samples to the nearest cluster center Update the cluster centers by calculating the average output of each class
- 8: **end while**
- 9: **Generate Multi-State Probability Model:**
- 10: Calculate state probabilities and construct the model.
- 11: **Evaluate and Iterate:**
- 12: Compute maximum error. If within limits, **End Algorithm**. Otherwise,
- 13: Increment N_p if $N_p < N_{\max}$, or reset N_p to 1 and increment N_c , then repeat from Step 4.

$$w_j[\tau + 1] = \left(\frac{1}{1 + d_j} \right) B_{O_j} a[\tau + 1] \quad \forall j \in I \cup K \quad (\text{C.3})$$

where communicate $w_j[\tau + 1]$ for all $j \in I \cup K$

$$\nu_j[\tau + 1] = \nu_j[\tau] + \rho w_j[\tau + 1] \quad \forall j \in I \cup K \quad (\text{C.4})$$

where $d_j \triangleq |N_j|$ represents the in-degree of atom-j in the directed graph described by the incidence matrix B.

Appendix D. PAC convergence plots for sub-problem P2 analysis

See Fig. D.17.

Data availability

Data will be made available on request.

References

- [1] Soto EA, Bosman LB, Wollega E, Leon-Salas WD. Peer-to-peer energy trading: A review of the literature. *Appl Energy* 2021;283:116268.
- [2] Tushar W, Saha TK, Yuen C, Smith D, Poor HV. Peer-to-peer trading in electricity networks: An overview. *IEEE Trans Smart Grid* 2020;11(4):3185–200. <http://dx.doi.org/10.1109/TSG.2020.2969657>.
- [3] Zhou Y, Wu J. Peer-to-peer energy trading in microgrids and local energy systems. In: Jenkins N, editor. *Microgrids and local energy systems*. Rijeka: IntechOpen; 2021. <http://dx.doi.org/10.5772/intechopen.99437>.
- [4] Wei X, Xu Y, Sun H, Chan WK. Peer-to-peer energy trading of carbon-aware prosumers: An online accelerated distributed approach with differential privacy. *IEEE Trans Smart Grid* 2024;15(6):5595–609. <http://dx.doi.org/10.1109/TSG.2024.3398041>.
- [5] Wang B, Xu L, Wang J. A privacy-preserving trading strategy for blockchain-based P2P electricity transactions. *Appl Energy* 2023;335:120664. <http://dx.doi.org/10.1016/j.apenergy.2023.120664>, URL <https://www.sciencedirect.com/science/article/pii/S0306261923000284>.
- [6] Anoh K, Maharjan S, Ikpehai A, Zhang Y, Adebisi B. Energy peer-to-peer trading in virtual microgrids in smart grids: A game-theoretic approach. *IEEE Trans Smart Grid* 2020;11(2):1264–75. <http://dx.doi.org/10.1109/TSG.2019.2934830>.
- [7] Yan M, Shahidehpour M, Paaso A, Zhang L, Alabdulwahab A, Abusorrah A. Distribution network-constrained optimization of peer-to-peer transactive energy trading among multi-microgrids. *IEEE Trans Smart Grid* 2021;12(2):1033–47. <http://dx.doi.org/10.1109/TSG.2020.3032889>.
- [8] Li P, Sheng W, Duan Q, Liang J, Zhu C. Day-ahead P2P energy sharing strategy among energy hubs considering flexibility of energy storage and loads. *CSEE J Power Energy Syst* 2024;10(3):1105–18. <http://dx.doi.org/10.17775/CSEEJPES.2021.06510>.

- [9] Zheng B, Wei W, Chen Y, Wu Q, Mei S. A peer-to-peer energy trading market embedded with residential shared energy storage units. *Appl Energy* 2022;308. <http://dx.doi.org/10.1016/j.apenergy.2021.118400>.
- [10] Fan W, Fan Y, Yao X, Yi B, Jiang D, Wu L. Distributed transaction optimization model of multi-integrated energy systems based on nash negotiation. *Renew Energy* 2024;225. <http://dx.doi.org/10.1016/j.renene.2024.120196>.
- [11] Huang D-W, Luo F, Bi J. Uncertainty-aware prosumer coalitional game for peer-to-peer energy trading in community microgrids. *Int J Electr Power Energy Syst* 2024;159. <http://dx.doi.org/10.1016/j.ijepes.2024.110021>.
- [12] Wang L, Zhou Q, Xiong Z, Zhu Z, Jiang C, Xu R, Li Z. Security constrained decentralized peer-to-peer transactive energy trading in distribution systems. *CSEE J Power Energy Syst* 2022;8(1):188–97. <http://dx.doi.org/10.17775/CSEEJPES.2020.06560>.
- [13] Tengfei M, Wei P, Hao X, Dexin L, Xiangyu L, Kai H. Cooperative operation method of wind solar hydrogen multi agent energy system based on Nash negotiation theory. *Chin J Electr Eng* 2021;41(01):25–39+395. <http://dx.doi.org/10.13334/j.0258-8013.psee.200956>.
- [14] Sheng H, Wang C, Dong X, Meng K, Dong Z. Incorporating P2P trading into DSO's decision-making: A DSO-prosumers cooperated scheduling framework for transactive distribution system. *IEEE Trans Power Syst* 2023;38(3):2362–75. <http://dx.doi.org/10.1109/TPWRS.2022.3187191>.
- [15] Zhong W, Xie S, Xie K, Yang Q, Xie L. Cooperative P2P energy trading in active distribution networks: An MILP-based Nash bargaining solution. *IEEE Trans Smart Grid* 2021;12(2):1264–76. <http://dx.doi.org/10.1109/TSG.2020.3031013>.
- [16] Chen Y, Pei W, Ma T, Xiao H. Asymmetric Nash bargaining model for peer-to-peer energy transactions combined with shared energy storage. *Energy* 2023;278(B). <http://dx.doi.org/10.1016/j.energy.2023.127980>.
- [17] Wang H, Huang J. Incentivizing energy trading for interconnected microgrids. *IEEE Trans Smart Grid* 2018;9(4):2647–57. <http://dx.doi.org/10.1109/TSG.2016.2614988>.
- [18] Patari N, Venkataraman V, Srivastava A, Molzahn DK, Li N, Annaswamy A. Distributed optimization in distribution systems: Use cases, limitations, and research needs. *IEEE Trans Power Syst* 2022;37(5):3469–81. <http://dx.doi.org/10.1109/TPWRS.2021.3132348>.
- [19] Feng C, Liang B, Li Z, Liu W, Wen F. Peer-to-peer energy trading under network constraints based on generalized fast dual ascent. *IEEE Trans Smart Grid* 2023;14(2):1441–53. <http://dx.doi.org/10.1109/TSG.2022.3162876>.
- [20] Zhou X, Liu Z, Zhao C, Chen L. Accelerated voltage regulation in multi-phase distribution networks based on hierarchical distributed algorithm. *IEEE Trans Power Syst* 2020;35(3):2047–58. <http://dx.doi.org/10.1109/TPWRS.2019.2948978>, American Control Conference, Philadelphia, PA, JUL 10-12, 2019.
- [21] Erseghe T. Distributed optimal power flow using ADMM. *IEEE Trans Power Syst* 2014;29(5):2370–80. <http://dx.doi.org/10.1109/TPWRS.2014.2306495>.
- [22] Wang Y, Nguyen T-L, Xu Y, Tran Q-T, Caire R. Peer-to-peer control for networked microgrids: Multi-layer and multi-agent architecture design. *IEEE Trans Smart Grid* 2020;11(6):4688–99. <http://dx.doi.org/10.1109/TSG.2020.3006883>.
- [23] Li J, Zhang C, Xu Z, Wang J, Zhao J, Zhang Y-JA. Distributed transactive energy trading framework in distribution networks. *IEEE Trans Power Syst* 2018;33(6):7215–27. <http://dx.doi.org/10.1109/TPWRS.2018.2854649>.
- [24] Wei X, Liu J, Xu Y, Sun H. Virtual power plants peer-to-peer energy trading in unbalanced distribution networks: A distributed robust approach against communication failures. *IEEE Trans Smart Grid* 2024;15(2):2017–29. <http://dx.doi.org/10.1109/TSG.2023.3308101>.
- [25] Ullah MH, Park J-D. Peer-to-peer energy trading in transactive markets considering physical network constraints. *IEEE Trans Smart Grid* 2021;12(4):3390–403. <http://dx.doi.org/10.1109/TSG.2021.3063960>.
- [26] Meng Y, Ma G, Ye Y, Yao Y, Li W, Li T. Design of P2P trading mechanism for multi-energy prosumers based on generalized nash bargaining in GCT-CET market. *Appl Energy* 2024;371. <http://dx.doi.org/10.1016/j.apenergy.2024.123640>.
- [27] Romvary JJ, Ferro G, Haider R, Annaswamy AM. A proximal atomic coordination algorithm for distributed optimization. *IEEE Trans Autom Control* 2022;67(2):646–61. <http://dx.doi.org/10.1109/TAC.2021.3053907>.
- [28] Haider R, Baros S, Wasa Y, Romvary J, Uchida K, Annaswamy AM. Toward a retail market for distribution grids. *IEEE Trans Smart Grid* 2020;11(6):4891–905. <http://dx.doi.org/10.1109/TSG.2020.2996565>.
- [29] Zakaria A, Ismail FB, Lipu MH, Hannan M. Uncertainty models for stochastic optimization in renewable energy applications. *Renew Energy* 2020;145:1543–71. <http://dx.doi.org/10.1016/j.renene.2019.07.081>, URL <https://www.sciencedirect.com/science/article/pii/S0960148119311012>.
- [30] Yang J, Su C. Robust optimization of microgrid based on renewable distributed power generation and load demand uncertainty. *Energy* 2021;223. <http://dx.doi.org/10.1016/j.energy.2021.120043>.
- [31] Zhai J, Wang S, Guo L, Jiang Y, Kang Z, Jones CN. Data-driven distributionally robust joint chance-constrained energy management for multi-energy microgrid. *Appl Energy* 2022;326. <http://dx.doi.org/10.1016/j.apenergy.2022.119939>.
- [32] Guo Z, Pinson P, Chen S, Yang Q, Yang Z. Chance-constrained peer-to-peer joint energy and reserve market considering renewable generation uncertainty. *IEEE Trans Smart Grid* 2021;12(1):798–809. <http://dx.doi.org/10.1109/TSG.2020.3019603>.
- [33] Alizadeh A, Esfahani M, Dinar F, Kamwa I, Moeini A, Mohseni-Bonab SM, Busvelle E. A cooperative transactive multi-carrier energy control mechanism with P2P energy plus reserve trading using Nash bargaining game theory under renewables uncertainty. *Appl Energy* 2024;353(B). <http://dx.doi.org/10.1016/j.apenergy.2023.122162>.
- [34] Wei C, Shen Z, Xiao D, Wang L, Bai X, Chen H. An optimal scheduling strategy for peer-to-peer trading in interconnected microgrids based on RO and Nash bargaining. *Appl Energy* 2021;295. <http://dx.doi.org/10.1016/j.apenergy.2021.117024>.
- [35] Cui S, Wang Y-W, Xiao J-W, Liu N. A two-stage robust energy sharing management for prosumer microgrid. *IEEE Trans Ind Inform* 2019;15(5):2741–52. <http://dx.doi.org/10.1109/TII.2018.2867878>.
- [36] Zhang X, Ge S, Liu H, Zhou Y, He X, Xu Z. Distributionally robust optimization for peer-to-peer energy trading considering data-driven ambiguity sets. *Appl Energy* 2023;331. <http://dx.doi.org/10.1016/j.apenergy.2022.120436>.
- [37] Mohseni S, Pishvae MS. A robust programming approach towards design and optimization of microalgae-based biofuel supply chain. *Comput Ind Eng* 2016;100:58–71. <http://dx.doi.org/10.1016/j.cie.2016.08.003>, URL <https://www.sciencedirect.com/science/article/pii/S0360835216302698>.
- [38] Esfahani PM, Kuhn D. Data-driven distributionally robust optimization using the Wasserstein metric: performance guarantees and tractable reformulations. *Math Program* 2018;171(1–2):115–66. <http://dx.doi.org/10.1007/s10107-017-1172-1>.
- [39] Li J, Khodayar ME, Wang J, Zhou B. Data-driven distributionally robust optimization of P2P energy trading and network operation for interconnected microgrids. *IEEE Trans Smart Grid* 2021;12(6):5172–84. <http://dx.doi.org/10.1109/TSG.2021.3095509>.
- [40] Zheng X, Qu K, Lv J, Li Z, Zeng B. Addressing the conditional and correlated wind power forecast errors in unit commitment by distributionally robust optimization. *IEEE Trans Sustain Energy* 2021;12(2):944–54. <http://dx.doi.org/10.1109/TSTE.2020.3026370>.
- [41] Duan C, Fang W, Jiang L, Yao L, Liu J. Distributionally robust chance-constrained approximate AC-OPF with Wasserstein metric. *IEEE Trans Power Syst* 2018;33(5):4924–36. <http://dx.doi.org/10.1109/TPWRS.2018.2807623>.
- [42] Yao L, Wang X, Li Y, Duan C, Wu X. Distributionally robust chance-constrained AC-OPF for integrating wind energy through multi-terminal VSC-HVDC. *IEEE Trans Sustain Energy* 2020;11(3):1414–26. <http://dx.doi.org/10.1109/TSTE.2019.2927135>.
- [43] Zhou A, Yang M, Zheng X, Yin S. Distributionally robust unit commitment considering unimodality-skewness information of wind power uncertainty. *IEEE Trans Power Syst* 2023;38(6):5420–31. <http://dx.doi.org/10.1109/TPWRS.2022.3230320>.
- [44] Zhong J, Li Y, Wu Y, Cao Y, Li Z, Peng Y, Qiao X, Xu Y, Yu Q, Yang X, Li Z, Shahidehpour M. Optimal operation of energy hub: An integrated model combined distributionally robust optimization method with Stackelberg game. *IEEE Trans Sustain Energy* 2023;14(3):1835–48. <http://dx.doi.org/10.1109/TSTE.2023.3252519>.
- [45] Zheng W, Huang W, Hill DJ, Hou Y. An adaptive distributionally robust model for three-phase distribution network reconfiguration. *IEEE Trans Smart Grid* 2021;12(2):1224–37. <http://dx.doi.org/10.1109/TSG.2020.3030299>.
- [46] Siqin Z, Niu D, Li M, Gao T, Lu Y, Xu X. Distributionally robust dispatching of multi-community integrated energy system considering energy sharing and profit allocation. *Appl Energy* 2022;321. <http://dx.doi.org/10.1016/j.apenergy.2022.119202>.
- [47] Zheng W, Wu W, Zhang B, Sun H, Liu Y. A fully distributed reactive power optimization and control method for active distribution networks. *IEEE Trans Smart Grid* 2016;7(2, SI):1021–33. <http://dx.doi.org/10.1109/TSG.2015.2396493>.
- [48] Le J, Liao X, Zhang L, Mao T. Distributionally robust chance constrained planning model for energy storage plants based on Kullback-Leibler divergence. *Energy Rep* 2021;7:5203–13. <http://dx.doi.org/10.1016/j.egy.2021.08.116>.
- [49] Zhou Y, Wang J, Zhang Y, Wei J, Sun W, Wang J. A fully-decentralized transactive energy management under distribution network constraints via peer-to-peer energy trading. *IEEE Trans Energy Mark Policy Regul* 2023;1(4):297–309. <http://dx.doi.org/10.1109/TEMPR.2023.3263685>.
- [50] Kumar D, Padhy BP. Optimal selection of voltage controlling parameter in uncertain active distribution network. *IEEE Trans Ind Appl* 2024;60(1):1576–88. <http://dx.doi.org/10.1109/TIA.2023.3324897>.
- [51] Zou K, Agalgaonkar AP, Muttaqi KM, Perera S. Distribution system planning with incorporating DG reactive capability and system uncertainties. *IEEE Trans Sustain Energy* 2012;3(1):112–23. <http://dx.doi.org/10.1109/TSTE.2011.2166281>.
- [52] Jiang R, Guan Y. Data-driven chance constrained stochastic program. *Math Program* 2016;158(1–2):291–327. <http://dx.doi.org/10.1007/s10107-015-0929-7>.
- [53] Cao Y, Wei W, Mei S, Shafie-Khah M, Catalao JPS. Analyzing and quantifying the intrinsic distributional robustness of cvar reformulation for chance-constrained stochastic programs. *IEEE Trans Power Syst* 2020;35(6):4908–11. <http://dx.doi.org/10.1109/TPWRS.2020.3021285>.
- [54] Song Z, Feng H, Chen X, Zhang H, Zhan Z, Xu Y. Low-carbon scheduling strategy of distributed energy resources based on node carbon intensity for distribution networks. *High Volt Eng* 2023;49(6):2318–28, URL <https://doi.org/10.1002/hve.202300006>.

- [55] Lee J-O, Kim Y-S. Novel battery degradation cost formulation for optimal scheduling of battery energy storage systems. *Int J Electr Power Energy Syst* 2022;137. <http://dx.doi.org/10.1016/j.ijepes.2021.107795>.
- [56] Lou C, Yang J, Fuentes EV, Zhou Y, Min L, Yu J, Meena NK. Power flow traceable P2P electricity market segmentation and cost allocation. *Energy* 2024;290. <http://dx.doi.org/10.1016/j.energy.2023.130120>.
- [57] Pepermans G, Driesen J, Haeseldonckx D, Belmans R, D'haeseleer W. Distributed generation: definition, benefits and issues. *Energy Policy* 2005;33(6):787–98. <http://dx.doi.org/10.1016/j.enpol.2003.10.004>.
- [58] Shi M, Wang H, Xie P, Lyu C, Jian L, Jia Y. Distributed energy scheduling for integrated energy system clusters with peer-to-peer energy transaction. *IEEE Trans Smart Grid* 2023;14(1):142–56. <http://dx.doi.org/10.1109/TSG.2022.3197435>.
- [59] Ferro G, Robba M, Haider R, Annaswamy AM. A distributed-optimization-based architecture for management of interconnected energy hubs. *IEEE Trans Control Netw Syst* 2022;9(4):1704–16. <http://dx.doi.org/10.1109/TCNS.2022.3165022>.
- [60] Development N, Commission R, Administration NE. Two departments notice on the implementation plan for solving the issues of abandoned water, wind, and solar energy. 2017, URL https://www.gov.cn/xinwen/2017-11/14/content_5239536.htm. [Accessed 17 August 2024].
- [61] Ministry of Ecology and Environment of the People's Republic of China, National Bureau of Statistics. Announcement on the release of the 2021 power sector CO2 emission factors. 2024, URL https://www.mee.gov.cn/xxgk2018/xxgk/xxgk01/202404/t20240412_1070565.html. [Accessed 12 August 2024].
- [62] Chen Y, Wen J, Cheng S. Probabilistic load flow method based on nataf transformation and latin hypercube sampling. *IEEE Trans Sustain Energy* 2013;4(2):294–301. <http://dx.doi.org/10.1109/TSTE.2012.2222680>.
- [63] Shu Z, Jirutitijaroen P. Latin hypercube sampling techniques for power systems reliability analysis with renewable energy sources. *IEEE Trans Power Syst* 2011;26(4):2066–73. <http://dx.doi.org/10.1109/TPWRS.2011.2113380>.
- [64] Zhao J, Wu Q, Hatziaargyriou ND, Li F, Teng F. Decentralized data-driven load restoration in coupled transmission and distribution system with wind power. *IEEE Trans Power Syst* 2021;36(5):4435–44. <http://dx.doi.org/10.1109/TPWRS.2021.3063114>.
- [65] Xiao D, Chen H, Cai W, Wei C, Zhao Z. Integrated risk measurement and control for stochastic energy trading of a wind storage system in electricity markets. *Prot Control Mod Power Syst* 2023;8(1). <http://dx.doi.org/10.1186/s41601-023-00329-3>.
- [66] Lu S, Lou G, Gu W, Zhang S, Yuan X, Li Q, Han H. Optimal dispatch for flexible uncertainty sets in multi-energy systems: An IGDT based two-stage decision framework. *CSEE J Power Energy Syst* 2023;9(6):2374–85. <http://dx.doi.org/10.17775/CSEEJPES.2020.07150>.
- [67] Makhdoumi A, Ozdaglar A. Convergence rate of distributed ADMM over networks. *IEEE Trans Autom Control* 2017;62(10):5082–95. <http://dx.doi.org/10.1109/TAC.2017.2677879>.